

UNCLASSIFIED

---

---

AD 257 735

*Reproduced  
by the*

ARMED SERVICES TECHNICAL INFORMATION AGENCY  
ARLINGTON HALL STATION  
ARLINGTON 12, VIRGINIA



---

---

UNCLASSIFIED

NOTICE: When government or other drawings, specifications or other data are used for any purpose other than in connection with a definitely related government procurement operation, the U. S. Government thereby incurs no responsibility, nor any obligation whatsoever; and the fact that the Government may have formulated, furnished, or in any way supplied the said drawings, specifications, or other data is not to be regarded by implication or otherwise as in any manner licensing the holder or any other person or corporation, or conveying any rights or permission to manufacture, use or sell any patented invention that may in any way be related thereto.

257735

205800

AFOSR-~~4~~ 593

COLUMBIA UNIVERSITY IN THE CITY OF NEW YORK

Solid State Sciences Division

Air Force Office of Scientific Research

Air Research and Development Command

Washington 25, D. C.

DEFORMATION AND FRACTURE  
OF  
CADMIUM AND CADMIUM-MAGNESIUM ALLOYS

Norman S. Stoloff

April  
1961

Contract No. AF49(638)-408

CATALOGED BY ASTIA  
AS AD NO.

NOX

"Qualified requestors may obtain copies of this report from the Armed Services Technical Information Agency (ASTIA), Document Service Center Arlington Hall Station, Arlington 12, Virginia. Department of Defense contractors must have their project or contract."

\$10.10

ASTIA  
JUN 15 1961  
TIPOR

257735

205 800

AFOSR-~~59~~ 593

COLUMBIA UNIVERSITY IN THE CITY OF NEW YORK

Solid State Sciences Division

Air Force Office of Scientific Research

Air Research and Development Command

Washington 25, D. C.

DEFORMATION AND FRACTURE  
OF  
CADMIUM AND CADMIUM-MAGNESIUM ALLOYS

Norman S. Stoloff

April  
1961

Contract No. AF49(638)-408

CATALOGED BY ASTIA

AS AD No.

NOX

"Qualified requestors may obtain copies of this report from the Armed Services Technical Information Agency (ASTIA), Document Service Center Arlington Hall Station, Arlington 12, Virginia. Department of Defense contractors must have their project or contract."

\$10.10

ASTIA  
JUN 15 1961  
TIPOR

## TABLE OF CONTENTS

	Page
I INTRODUCTION	1
A. Purpose of Investigation	1
B. Previous Work	1
C. Role of Axial Ratio	5
D. Effect of Alloying Elements	7
E. Outline of Investigation	8
II EXPERIMENTAL PROCEDURES	9
A. Polycrystalline Cadmium	9
B. Polycrystalline Cadmium-Magnesium Alloys	12
C. Single Crystals	14
III EXPERIMENTAL RESULTS	18
A. Deformation and Fracture of Polycrystalline Cadmium	18
1. Stress-Strain Behavior	18
2. Fracture Behavior	20
3. Other Aspects of Deformation Behavior	22
4. Microstructural Observations	23
B. Deformation and Fracture of Polycrystalline Cd-Mg Alloys	27
1. Stress-Strain Behavior	27
2. Strength vs. Temperature and Alloy Content	29
3. Fracture Behavior	30
4. Microstructural Observations	31
5. Compression Tests	35
C. Twinning and Non-Basal Slip in Single Crystals	37
1. Twinning in Tension	37
2. Non-Basal Slip in Compression	39
3. Non-Basal Slip in Bending	42
4. Further Observations of Non-Basal Slip	43
IV DISCUSSION	45
A. Deformation of Polycrystalline Aggregates	45
B. Ductility Transition in Hexagonal Metals	51
C. Cleavage in Metals	56
D. Non-Basal Slip	63

TABLE OF CONTENTS (Continued)

V	SUMMARY AND CONCLUSIONS	67
VI	SUGGESTIONS FOR FUTURE WORK	71
VII	ACKNOWLEDGMENTS	72
	BIBLIOGRAPHY	74

## I INTRODUCTION

### A. Purpose of Investigation

Although numerous studies have been made of the mechanical properties of cadmium single crystals, no comprehensive investigation of deformation and fracture in polycrystalline cadmium has been carried out. This investigation was initiated to determine the mechanisms of deformation and fracture in polycrystalline cadmium, and to attempt to correlate these mechanisms with pertinent aspects of single crystal behavior. A second objective of this work was to determine whether the slip systems and mode of fracture of polycrystalline cadmium could be altered by reduction of the axial ratio, which is 1.886, through alloying. This is of interest because zinc, with virtually the same axial ratio as cadmium, exhibits brittle cleavage at room temperature and below, while cadmium remains ductile to 4.2<sup>1</sup> K. An understanding of the factors giving rise to ductile failure in cadmium would be useful in developing means for alleviating brittleness in other materials of hexagonal close packed or body centered cubic structure.

### B. Previous Work

Many investigations of plastic deformation in cadmium

single crystals were carried out about 30 years ago, and the results have been summarized by Schmid and Boas.<sup>1</sup> The slip and twinning systems were established as  $(0001) \langle 11\bar{2}0 \rangle$  and  $\{10\bar{1}2\} \langle 10\bar{1}1 \rangle$  respectively.<sup>1</sup> Cadmium was found to obey a critical resolved shear stress law for basal glide.<sup>1,2</sup> The shape of the entire stress strain curve was found to depend on crystal orientation, with a minimum rate of work hardening for crystals oriented with  $\chi_0^*$  near  $45^\circ$ . The yield stress for basal glide was not appreciably affected by temperature. Decreasing the temperature from room temperature to  $4.2^\circ \text{K}$ <sup>1</sup> barely doubled the yield stress.

Twinning becomes the preferred deformation mode for crystals originally oriented with  $\chi_0$  near  $0^\circ$ , or for crystals which have deformed enough to bring a twinning plane into favorable orientation. The higher is  $\chi_0$ , the greater is the amount of slip which occurs before the lattice rotates sufficiently for twinning to begin. Twinning therefore acts as a limit to the amount of slip deformation which may occur. Secondary basal glide subsequently develops within the twins, resulting in marked necking and finally rupture of the crystal.

Recently Thompson and Millard<sup>3</sup> tested crystals oriented

---

\*  $\chi_0$  is the angle between the specimen axis and the line of maximum slope in the basal plane.



with  $\chi_0 < 5^\circ$ , and claimed to have established a critical resolved shear stress law for twinning in cadmium. Later work by Thompson and Hingley<sup>4</sup> indicated that a law of this type probably applies only to the propagation of twin nuclei, rather than for the introduction of twins into an untwinned lattice.

Another important deformation mode for cadmium is kinking, which usually occurs in compression but may appear in tension as well. Kink bands are a simple type of deformation band<sup>5</sup>. Plastic flow is confined almost entirely to the regions within a band, and causes severe but regular bending of the glide lamellae around an axis that initially is in the slip plane and normal to the slip direction.

Several reports of non-basal slip in cadmium have appeared in the literature recently, two of the reports having appeared after work on this project was in progress. Brown<sup>6</sup> reported cross slip on electron micrographs, but did not identify the cross-slip plane. Wernick and Thomas<sup>7</sup> observed non-basal slip traces parallel to  $[\bar{1}\bar{1}2\bar{3}]$  on a crystal bent with a pair of tweezers, but this too was an isolated observation, with no confirmation of the glide plane. The critical stress for pyramidal glide, and the temperature and strain rate dependence of glide on this system were not discussed. Price<sup>8</sup> has reported some observations of non-basal slip in thin films

of cadmium with the aid of transmission electron microscopy, but a full publication of these observations was not available at this writing.

Pyramidal  $\{11\bar{2}2\} \langle 11\bar{2}3 \rangle$  slip also has been observed on zinc single crystals<sup>9,10</sup> and  $\{11\bar{2}2\} \langle 10\bar{1}0 \rangle$  slip on magnesium single crystals,<sup>11</sup> all oriented with the basal plane nearly parallel to the specimen axis. These reports provided the original motivation to attempt to establish the existence of a pyramidal slip system in cadmium.

Very little work has been reported on the fracture of cadmium, with the exception of some single crystal data. Single crystals exhibited glide strains of 400 per cent at room temperature, and 80 per cent at 4.2 K.<sup>1</sup> Failure in every reported case was by necking down and shearing off of the crystal. Cleavage in cadmium single crystals has never been observed.

Magnusson and Baldwin<sup>12</sup> reported a ductile to brittle transition for polycrystalline cadmium at about  $-160^{\circ}\text{C}$ . for specimens tested at 0.05 in./in./min. in tension. However, even at  $-196^{\circ}\text{C}$ . substantial ductility was retained. The transition temperature was strain rate dependent, impact loading at 19,000 in./in./min. raising the transition temperature to about  $-85^{\circ}\text{C}$ . No information was given on microstructures or

fracture appearances of test specimens, nor was there any discussion of stress strain behavior, work hardening characteristics or tensile strength as functions of temperature. Since these data are necessary for a full understanding of the fracture mechanism in cadmium, the first aim of the present investigation was to obtain this information.

### C. Role of Axial Ratio

The hexagonal metals are usually discussed in terms of their axial ratios, 1.633 being the ideal ratio for close packing of hard spheres. Cadmium has the highest  $c/a$  ratio of all common hexagonal metals, 1.886. The only other hexagonal metal with  $c/a$  higher than the ideal is zinc: 1.856. Those with  $c/a$  ratios below the ideal include magnesium: 1.623, titanium: 1.587, zirconium: 1.585, rhenium: 1.58 and beryllium: 1.565.

In general, the lower the  $c/a$  ratio, the more complex the observed deformation behavior. A summary of observed slip and twinning systems in the hexagonal metals appears in Table 1. For zinc and cadmium, the commonly observed deformation modes are (0001) slip and  $\{10\bar{1}2\}$  twinning.<sup>1</sup> However, zinc also exhibits pyramidal  $\{11\bar{2}2\}$  slip at room temperature and lower temperatures,<sup>9,10</sup> and prismatic  $\{10\bar{1}0\}$  slip at elevated temperatures.<sup>13</sup> For those metals with  $c/a$  below the ideal, additional slip modes appear, and many new twinning

14-16  
modes as well.

The importance of the  $c/a$  ratio seems to lie in its influence on atomic densities and interplanar spacings. In almost every case the commonly observed slip plane is the one with highest packing density and largest interplanar spacing.<sup>17</sup>

Consideration of interplanar spacings for the various planes results in some uncertainty, however, in the general applicability of this rule. Because of the presence of the centered atoms the hexagonal close packed structure may be considered as being composed of two interpenetrating simple hexagonal lattices.<sup>17</sup> If a hexagonal lattice is viewed in a  $\langle 11\bar{2}0 \rangle$  direction, the basal planes are uniformly spaced at intervals of  $c/2$ , but other possible slip planes are not. The ratios of non-uniform spacings for the  $(10\bar{1}0)$ ,  $(10\bar{1}1)$  and  $(10\bar{1}2)$  planes are  $1/3:2/3$ ,  $1/6:5/6$  and  $1/3:2/3$ , respectively.<sup>17</sup> The effective spacing in such situations is smaller than it would be for one of the primitive lattices, and slip is more difficult. Consequently in addition to the surface atomic density for a plane, the non-uniform interplanar spacing must also be taken into account as a factor in determining the operative slip plane. Even on this basis however  $\{11\bar{2}2\}$  is an unlikely slip system for cadmium

and zinc.

The axial ratio also is of importance in determining the operative twin system in the hexagonal metals. Again, the lower the axial ratio, the more likely that  $\{10\bar{1}2\}$  twinning will be replaced by another mode. Also, depending on whether the  $c/a$  ratio is less or greater than the value 1.732, there results an extension ( $<1.732$ ) or a compression ( $>1.732$ ) in<sup>18</sup> the direction of the  $c$  axis when a  $\{10\bar{1}2\}$  twin is formed. Thus for zinc and cadmium, twinning on the  $\{10\bar{1}2\}$  planes cannot occur in compression when the basal plane is either parallel to or slightly inclined to the stress axis, although twinning is the primary deformation mode in tension for crystals of this orientation.

#### D. Effect of alloying Elements

Substitutional alloying elements sometimes drastically change the  $c/a$  ratio of the base metal, as is the case for lithium in magnesium.<sup>19</sup> This may allow new slip planes to act, as the atomic densities of the various possible slip planes are altered. Thus magnesium - 14 per cent lithium alloys exhibit far more prismatic  $\{10\bar{1}0\}$  slip than does unalloyed magnesium,<sup>19</sup> presumably due to the reduction in axial ratio. Trace impurities also have been known to alter slip

behavior. The presence of nitrogen in cadmium causes basal glide bands to cluster after small deformations.<sup>20</sup> The presence of 0.5 per cent cadmium in zinc increases the relative amount of twinning compared to slip.<sup>21</sup> The primary slip system in titanium appears to depend on oxygen content.<sup>22</sup> Very few observations exist, however, on the effect of alloying elements on twin formation.<sup>21</sup>

The only element which is known to be highly soluble in cadmium is magnesium.<sup>23</sup> A complete range of solid solutions exists above 253°C, but at room temperature superlattices corresponding to  $MgCd_3$ ,  $MgCd$  and  $Mg_3Cd$  are formed.<sup>24,25</sup> Axial ratios at 310°C for cadmium-rich alloys were determined by Hume-Rothery and Raynor,<sup>25</sup> who found that magnesium sharply reduces the axial ratio of cadmium, particularly at low solute concentrations. At room temperature magnesium is soluble in cadmium only to about 16 atomic per cent.<sup>24</sup> Beyond this concentration, the superlattice  $MgCd_3$  coexists with the primary solid solution. Similarly, for higher magnesium contents, the superlattices  $MgCd$  and  $MgCd_3$  coexist at room temperature.<sup>24</sup>

#### E. Outline of Present Investigation

Several aspects of the deformation and fracture behavior of cadmium were planned for study, and they may conveniently be divided into three groups:

- 1) Deformation and fracture of polycrystalline cadmium
- 2) Deformation and fracture of polycrystalline cadmium-magnesium alloys.
- 3) Twinning and non-basal slip in cadmium single crystals and coarse grained polycrystals.

Tensile tests were carried out on polycrystalline cadmium and cadmium-magnesium alloys to determine flow stresses, work-hardening behavior, fracture strength and fracture ductility. Variables employed in this investigation included temperature, alloy content (and c/a ratio) and grain size. Some compression data also have been obtained for comparison purposes. Twinning and non-basal slip in single crystals were studied in tension, compression and bending over a wide temperature range. The results were then analyzed in terms of existing models for plastic deformation and fracture in metals of hexagonal close packed structure.

## II EXPERIMENTAL PROCEDURES

### A. Polycrystalline Cadmium

Two purities of cadmium were employed for deformation and fracture studies on polycrystals. Cadmium of 99.95 per

cent purity was supplied by Belmont Smelting and Refining Co. Cadmium of 99.99+ per cent purity was supplied by American Smelting and Refining Co. Spectrographic analyses are given in Table 2. As received bars were cold swaged from 1/2 in. round and 3/8 in. round (for the 2 purities respectively) to 0.187 in. round. Threaded cylindrical tensile specimens were machined from the 0.187 in. bars to give approximately a 1/2 in. long straight gage section with a reduced diameter of about 0.110 in. Specimens were then sealed in evacuated pyrex capsules and heat treated in the range 140-280 °C to produce desired grain sizes. All specimens were furnace cooled to room temperature, at a rate of about 100 °C/hour, and broken out of their capsules. Average grain diameters were determined by etching in a 10 per cent nitric acid solution and counting grains longitudinally under a tool-maker's microscope. All grain size counts were made at a minimum of 3 places along the specimen gage length, and averaged. These values were substantially the same as those taken on transverse sections of the specimens. All specimens were then polished in a solution containing 320g CrO<sub>3</sub> and 20g Na<sub>2</sub> SO<sub>4</sub> in 1000 cc of H<sub>2</sub>O. This solution sometimes left a brown stain on the specimen. When this occurred a further polish was given with a solution of 1 part HNO<sub>3</sub> and 2 parts H<sub>2</sub>O<sub>2</sub> in 2 parts ethyl alcohol.<sup>26</sup> Minimum diameters and gage lengths were measured



optically with the tool-maker's microscope. Readings could be taken to the nearest 0.0001 in., but variations in readings from place to place along the specimen probably placed the final accuracy at about 0.001 in.

Tensile testing was carried out on a screw-driven Instron machine, at a constant rate of crosshead movement, which for most tests was 0.01 in./in./min. Load vs. time, and therefore load vs total strain were recorded on a synchronous chart. Temperatures from  $-196^{\circ}\text{C}$  to  $-40^{\circ}\text{C}$  were obtained by passing nitrogen gas through a copper coil immersed in liquid nitrogen, and then feeding the gas into a jacket around the specimen. Tests at  $4.2^{\circ}\text{K}$  were carried out in a helium cryostat, at a crosshead rate of 0.1 in./in./min.

The strain readings in the "elastic" range were valueless due to the softness of the machine. However, plastic strains measured from the yield stress to the end of test checked well with optical measurements of the final strain. Most of the data are reported in terms of engineering stress and strain. Up to the point of necking, these values do not differ much from true-stress strain values, as checked by calculations. The form of the stress-strain curve was not altered by using engineering values of stress and strain, although the apparent work hardening rate was too low.

Compression specimens were tested in a jig similar to

one designed by Gilman.<sup>9</sup> The jig was mounted on the under side of the Instron crosshead. Load was transmitted by means of a rod connected to a movable part of the jig at one end, and the load cell at the other end. A downward movement of the crosshead applied a compressive load to the specimen.

Fractured tensile specimens were measured optically with the tool-maker's microscope to give area at fracture and an estimate of total elongation. Fracture data were then plotted as a function of temperature or grain size.

Metallographic observations were carried out on the specimens using both normal and polarized light. No etching was necessary to reveal slip or twin traces on the polished surfaces.

#### B. Polycrystalline Cadmium-Magnesium Alloys

Cadmium bars of 99.99+ per cent purity were melted with magnesium bars of 99.97 per cent purity, supplied by the Dow Chemical Co., see Table 2 for analysis, to obtain a series of alloys up to 15.35 weight per cent magnesium. Melting was carried out in an induction unit under a dried argon atmosphere in zirconia crucibles. The alloys were kept molten for about 15 minutes to achieve homogeneity by magnetic stirring, and were cooled from the bottom with the aid of water

cooled jackets. A small pipe resulted, with a considerable amount of impurities concentrated near the top of the ingot. The ingots, usually weighing 200 to 300 grams and about  $4 \times \frac{3}{4}$  in. in diameter, were cropped to remove the pipe and contaminated portion. The ingots were then machined lightly to remove the surface, and enclosed in pyrex capsules. Homogenization treatments were carried out for two to four weeks at  $275^{\circ}\text{C}$ .

The ingots were reduced to  $\frac{3}{16}$  in. round by hot swaging at  $275\text{-}300^{\circ}\text{C}$  until the final pass, which was done cold. The surface periodically was chemically polished to minimize contamination of the melt. Chemical analyses were carried out by Lucius Pitkin and Co. for the per cent magnesium. A minimum of two analyses were made for each melt from different parts of the ingot. Samples were sent for analysis in capsules identified by a code number, and duplicate samples always checked well. Samples were dissolved immediately at Lucius Pitkin to avoid contamination from the air. The results of these analyses are presented in Table 3 in terms of average weight per cent and atomic per cent magnesium. Axial ratios for these alloys are estimated from data of Edwards et al<sup>24</sup> and Hume-Rothery and Raynor.<sup>25</sup> Procedures for specimen preparation were identical to those for unalloyed cadmium with the exception that the alloys were kept continuously under vacuum between machining, polishing and testing.

This was done because of the extreme reactivity of the alloys with the atmosphere. Chemically polished surfaces began to be contaminated by the atmosphere within a few minutes, although widespread attack usually occurred only after a period of hours. The time between polishing and testing therefore was kept to a minimum - usually about 1/2 hour. In any case several investigations have shown that surface coatings do not alter the mechanical properties of polycrystalline cadmium.<sup>27. 28</sup>

### C. Single Crystals

It was desired to obtain a large yield of single crystals oriented  $\chi_0 < 10^\circ$ , in order to be able to suppress basal slip during deformation by keeping the resolved shear stress on the basal plane to a minimum.

Cylindrical single crystals of cadmium were prepared by a seeding technique developed by Weiner<sup>29</sup> to obtain a predetermined orientation. A seed of 3/16 in. diameter and about 2 1/2 in. long of the desired orientation was placed beneath a polycrystalline rod of 3/16 in. diameter and about 10 in. long inside a pyrex tube coated with a fine layer of aquadag, a colloidal suspension of graphite. Two of these tubes in turn were placed within a vycor tube fitted with a stop-cock

to permit evacuation. The assembly was lowered vertically through a furnace with a narrow hot zone at about 400 C. Placement of the assembly so that only part of the seed would melt was sufficient to insure a carry-over of the orientation to the polycrystalline rod. Bicrystals and tricrystals were prepared by passing polycrystalline rods through the gradient without seeds.

The single crystal rods were sectioned to specimen size by an acid-cutting technique originally developed for zinc crystals.<sup>30</sup> An aqueous solution of nitric acid is the cutting agent. The acid is picked up by a plexiglass disc spinning through the acid which is contained in a sump-like arrangement. The disc is driven by a small motor powered through a variac so that the optimum cutting speed could be achieved. The section to be cut, the acid bath, and the spinning disc are enclosed in a plexiglass case.

The rod to be sectioned was coated with a thick layer of collodion. At the points at which sectioning was to be effected, the collodion was removed over a length of about 1/8 in. by dissolving it in acetone.

To prepare a surface suitable for microscopic examination, each crystal was chemically polished with the solutions

described previously for polycrystals.

Orientations of the crystals were determined by Laue back reflection X-ray patterns, either before test or after a small amount of strain, the latter situation allowing easier identification of the basal plane. (Cadmium cannot be cleaved along the basal plane, making it difficult to obtain X-ray diagrams of simple hexagonal symmetry). Some crystals were immersed in a solution of 1 per cent iodine in ethyl alcohol (by weight). Hexagonal pits resulted on 2 azimuths of the crystal, separated by  $180^{\circ}$ . X-ray analysis later showed that the faces on which these pits appeared were parallel to the basal planes. Therefore this served as a quick means of checking specimen orientation.

To avoid damage to the crystals before test, mechanical grips had to be avoided. Therefore brass grips were soldered onto tension specimens using ordinary 60-40 solder. No solder was necessary for compression specimens. In tension these grips were attached to universal joints either by pins or by screwing directly into the universal joints. In compression, shoulders on the grips gave a bearing surface for the transmittal of load. Specimens tested in tension had a uniform gage section between grips of about  $1/2$  in., while compression specimens were  $3/4$  to 1 in. long.

Elevated temperature tests in tension were carried out inside a Kanthal wound resistance furnace. Temperatures were measured by a thermocouple attached to the specimen. For low temperature tests, baths of dry-ice and acetone and liquid nitrogen were used to achieve temperatures of  $-77^{\circ}\text{C}$  and  $-196^{\circ}\text{C}$  respectively.

Bend tests also were carried out on cadmium single crystals and very coarse grained polycrystals. A four-point bending device was constructed which enabled deformation to be observed under a microscope, if desired. In order to induce non-basal slip, it was usually necessary to orient the crystal so that the bend axis was parallel to (0001).

Metallographic examination was carried out directly on the deformed specimens, the prior polish allowing easy resolution of deformation traces.

The orientation of slip and twinning traces on the cylindrical crystals used in this investigation were determined by a technique described by Barrett,<sup>15</sup> and recently employed by Schadler.<sup>31</sup> The orientation of the crystal was determined with respect to the specimen axis and a reference scratch by the Laue back-reflection X-ray technique. After straining, the specimen was mounted in a chuck on a microscope stage capable of being rotated through  $360^{\circ}$ . The

specimen was rotated in the chuck about its longitudinal axis, angular measurement being provided by a disc mounted concentric with the chuck. This angle, designated  $\alpha$ , was measured simultaneously with the angle  $\phi$  made by the slip or twin trace with respect to the longitudinal axis. The resulting values of  $\alpha$  and  $\phi$  were plotted on a stereographic projection of the crystal orientation, and the great circle passing through these points represented the trace of the observed plane. Slip directions were not measured directly, but rather were inferred from the intensity of slip traces at various azimuths of the crystal. For example, slip along  $\langle 11\bar{2}0 \rangle$  will result in no offset on the basal plane, since all  $\langle 11\bar{2}0 \rangle$  will be in the basal plane. On the other hand, slip along  $\langle 11\bar{2}\bar{3} \rangle$  will result in maximum offset on the basal plane, and none at  $90^\circ$  to the basal plane.

### III EXPERIMENTAL RESULTS

#### A. Deformation and Fracture of Polycrystalline Cadmium

##### 1. Stress-Strain Behavior

Tensile tests were carried out on specimens of several different grain sizes in the range  $-196^\circ\text{C}$  to room temperature, and at  $-269^\circ\text{C}$  (liquid helium). Pertinent data for these tests



are listed in Table 4 for 99.95 per cent cadmium and Table 5 for 99.99+ per cent cadmium. Typical stress-strain curves at several temperatures are shown in Fig. 1 for the 99.95 per cent cadmium. Fig. 2 shows the dependence of yield stress and flow stresses for 2, 5, 10, and 15 per cent plastic strain on temperature for specimens with grain sizes near 0.020 in.

Specimens tested at room temperature yielded with many sharp twinning bursts on the stress-strain curve. Twinning bursts continued to occur until the onset of necking, and were more pronounced for coarse grained material. As necking proceeded the load decreased until the specimen sheared off at the neck at zero load. This continual drop in load to zero during necking was noted in all specimens tested above  $-140^{\circ}\text{C}$ .

For tests at lower temperatures there was a gradual transition from complete necking to almost none below  $-180^{\circ}\text{C}$ . Similarly the extent of twinning on the stress-strain curve was vastly reduced at lower temperatures. Decreasing the grain size also tended to reduce the amount of twinning on the curves.

The work hardening behavior of polycrystalline cadmium was moderately temperature dependent as shown in Fig. 1. At room temperature the stress-strain curves showed a decrease

in slope with increasing strain. At lower temperatures the curves became more nearly linear until the onset of necking. Specimens tested at  $-196^{\circ}\text{C}$  and  $-269^{\circ}\text{C}$  showed almost perfectly linear stress-strain curves from the start of plastic deformation to just prior to fracture, when the load leveled off. Plotting the data on true stress-true strain coordinates did not alter the linearity of the curves. The average coefficient of work hardening in the nearly linear portions increased with decreasing temperature, but the effect was relatively small, the coefficient approximately doubling between room temperature and  $-196^{\circ}\text{C}$ .

## 2. Fracture Behavior

The suppression of necking with decreasing temperature is best described by a plot of per cent reduction in area at fracture vs. temperature, as shown in Fig. 3 for 99.95 per cent cadmium of several grain sizes. A sharp transition in ductility occurs at about  $-155^{\circ}\text{C}$ , independent of grain size. Reductions in area in the transition range for specimens of the purer cadmium listed in Table 5 agree well with those shown in Fig. 3. Magnusson and Baldwin<sup>12</sup> have presented an almost identical plot of reduction in area vs. temperature for commercially pure cadmium tested at a strain rate of 0.05 in./in./min. with the transition occurring at about  $-165^{\circ}\text{C}$ . An appreciable strain-rate effect also was reported, higher

strain rates causing an elevation in the transition temperature. However, the ductility at  $-196^{\circ}\text{C}$  was the same for each of four strain rates up to 19,000 in./in./min.

A plot of total plastic elongation at fracture vs. temperature also is presented in Fig. 3, and follows closely the curve for reduction in area. It is noteworthy that both curves show a ductility plateau from about  $-190^{\circ}\text{C}$  to  $-269^{\circ}\text{C}$ , at the relatively high level of about 15 per cent reduction in area or elongation. Therefore, this transition phenomenon in cadmium is not truly from ductile to brittle fracture but may more aptly be termed a ductile - "quasi brittle" transition. Attempts to induce more nearly brittle failure by employing circumferential notches and testing at a strain rate of 20 in./in./min. at  $-196^{\circ}\text{C}$  were unsuccessful. The ductility was substantially unaffected.

Accompanying the reduction in ductility with decreasing temperature is an increase in tensile strength, as shown in Fig. 4. Between room temperature and about  $-175^{\circ}\text{C}$  the tensile strength is not appreciably affected by grain size. There is a distinct grain size dependence below  $-175^{\circ}\text{C}$ , although the strength is approximately constant with temperature at constant grain size in the same range. At  $-196^{\circ}\text{C}$ , both the tensile strength and fracture strength (load at fracture

divided by cross sectional area at fracture) are approximately proportional to  $d^{-1/2}$ , where  $d$  is the average grain diameter. A plot of true fracture stress vs.  $d^{-1/2}$  is shown in Fig. 5 for 99.95 per cent cadmium. For comparison purposes, a similar plot is presented for 99.99 per cent zinc, which also had been tested at  $-196^{\circ}\text{C}$ . The higher strength of cadmium at each grain size is a consequence of the large amount of plastic deformation still occurring at  $-196^{\circ}\text{C}$ , compared to the almost completely brittle fracture of zinc. It is interesting that both curves extrapolate back to the origin, implying the relation for fracture stress:

$$\sigma_F = \sigma_0 + k d^{-1/2} \quad (1)$$

where  $k$  is a constant. This equation has previously been demonstrated for brittle fracture in iron,<sup>32</sup> zinc,<sup>32,33</sup> and magnesium,<sup>34</sup> and for ductile fracture in iron.<sup>35</sup> The value of  $k$  for cadmium is 3050, vs. 860 for zinc in units of (psi) in.<sup>1/2</sup>. The value for zinc is almost identical to that obtained by Greenwood and Quarrell.<sup>33</sup> The yield stress of cadmium, both at room temperature and at  $-196^{\circ}\text{C}$ , was found to obey a similar relation, with  $k = 560$  (psi) in.<sup>1/2</sup> at  $-196^{\circ}\text{C}$ , as shown in Fig. 6. The yield stress is much more dependent on grain size than on temperature, as Fig. 6 clearly shows.

### 3. Other Aspects of Deformation Behavior

Several compression tests on polycrystalline cadmium

confirmed the general trends of increasing strength with decreasing temperature. Most of this work was devoted to an analysis of microstructures, as described in the following section.

In order to determine the effect of recovery on the stress-strain behavior of cadmium, tests were carried out at room temperature and at  $-196^{\circ}\text{C}$  by interrupting deformation at an arbitrary strain, unloading and then reloading, after a 15 minute rest period. This is about the period of time necessary to run a continuous test to fracture at room temperature. At room temperature about 30 per cent recovery of the flow stress was achieved after 15 minutes, while at  $-196^{\circ}\text{C}$  only about 5 per cent recovery was achieved. This is in agreement with reports in the literature of the recovery behavior of cadmium<sup>1,33</sup> which show that recovery is negligible at  $-196^{\circ}\text{C}$ <sup>36</sup> relative to room and elevated temperatures. Seeger<sup>36</sup> states that the recovery range begins at about  $-50^{\circ}\text{C}$  for cadmium.

#### 4. Microstructural Observations

All fractured tensile specimens were examined for evidence of deformation markings, and certain selected specimens were examined just past their yield strains and after several per cent strain. Basal slip and twinning appeared in some grains of barely yielded specimens. With increasing deformation the number of grains with slip and twin markings increased, as did the density of deformation markings within grains

that had already yielded. Whether or not drops in load were observed on the stress-strain curve, twinning continued throughout each test, even at  $4.2^{\circ}\text{K}$ , as shown in the micrograph of Fig. 7. Basal slip within the twins also was noted, particularly in fractured specimens, down to  $4.2^{\circ}\text{K}$ .

The appearance of deformation twins was somewhat affected by temperature. As the temperature decreased they generally became somewhat narrower and were less likely to exhibit secondary basal slip. This is clearly seen in Figs. 8 and 9a, which compare specimens tested in compression at room temperature and  $-196^{\circ}\text{C}$  respectively. For a given strain, there was approximately the same density of twins at all temperatures. Kinking also was observed at all test temperatures.

At sub-transition temperatures, and particularly at  $-196^{\circ}\text{C}$ , many new markings appeared in the microstructures, as is shown in Fig 9b. Both tension and compression specimens exhibited the traces. Some doubt arose whether these markings were narrow twins or bands of slip on a new system. Polishing, however, removed these markings readily, while twin traces were made to stand out in relief by the polishing reagent. Other properties of these markings which indicate that they are slip traces are the following:

- 1) They are seen only at sub-transition temperatures, while

twins of finite thickness are observed at all test temperatures.

2) They do not react under polarized light, while ordinary twin traces react so as to stand out distinctly from the matrix.

3) They usually appear in clusters, while twins usually appear in small numbers, and widely separated.

4) They usually appear at angles of  $60-65^\circ$  with basal traces, which is about the range of angles that pyramidal  $\{10\bar{1}1\}$  or  $\{11\bar{2}2\}$  traces would make with the basal plane.

Stereographic analysis of these traces was not possible because of the relatively small grain size of the specimens, and their cylindrical shape, which ruled out two-surface analysis. Tests on single crystals and bicrystals reported in a later section indicate, however, that these traces arise from slip on pyramidal  $\{11\bar{2}2\}$  planes.

Much effort was devoted to examining fracture surfaces of tensile specimens for evidence of a change in fracture mode within the transition range. Above the transition range, where necking caused about 100 per cent reduction in area at fracture, the material actually failed by ductile shear along the slip planes. Within the transition range necking was interrupted by intergranular failure. Finally, below  $-180^\circ\text{C}$  necking was almost entirely suppressed, with grain boundary failure always intervening after considerable deformation

had occurred within the grains. No evidence of cleavage within the grains or in the boundaries ever was noted, even at  $4.2^{\circ}\text{K}$ .

Several specimens were tested at  $-196^{\circ}\text{C}$  to the point where the stress-strain curve started to level off, that is, just prior to fracture. Intergranular microcracks extending usually one or two grains in length were noted at the region where necking was beginning. Subsequent reloading of such specimens did not cause failure until considerable plastic strain was imposed. This clearly indicates the resistance to propagation of stopped intergranular cracks, in contrast to their relatively rapid propagation once the maximum load is reached during continuous testing.

Recrystallization during test at super-transition temperatures has been advanced as the cause of the ductile-brittle transition in pure magnesium.<sup>37</sup> Accordingly, several room temperature test specimens were examined just prior to fracture and just after fracture for evidence of recrystallization. No recrystallization ever was noted, nor was recrystallization noted immediately after testing at any lower temperature. However, fractured specimens allowed to stand at room temperature for several days began to exhibit very small recrystallized grains within the necked region.



## B. Deformation and Fracture of Polycrystalline Cadmium-Magnesium Alloys

Specimens of six polycrystalline cadmium-magnesium alloys, ranging in magnesium content from 1.96 to 15.35 weight per cent, see Table 3, were tested in tension in the range  $-169^{\circ}\text{C}$  to room temperature. Four of the alloys, melts I, III, IV and V contained less than 16 atomic per cent magnesium, and therefore may be presumed to be free from complications arising from order-disorder phenomena.<sup>24</sup> Melts II and VII, containing 19.4 and 45.6 atomic per cent magnesium respectively, usually were tested in the slow furnace cooled condition, and therefore were ordered. Several specimens of melt II, however, were tested in the water quenched condition, with no apparent effect on the test results. Electrical resistivity measurements carried out on samples of this alloy later showed that quenching does not suppress ordering. Tensile data for all the alloys are presented in Table 6. All subsequent references to these alloys will be in terms of weight per cent unless designated differently.

### 1. Stress-strain Behavior

The yield behavior of the alloys was strikingly different from that of pure cadmium in several respects. Whereas cadmium yielded rather abruptly over the entire temperature range (without a yield point), the alloys yielded more gradually,

particularly below the ductility transition range. Stress-strain curves at several temperatures for melt III are shown in Fig. 10. The gradual yielding made it more difficult to assign yield strengths to the alloys. This in part accounts for the scatter in yield strength with temperature for each of the alloys.

Specimens of melts III, IV and V exhibited the yield point phenomenon when tested at room temperature. The upper yield point was rounded, and there was only a small drop in load to the lower yield point. Yield points never were observed at lower temperatures. Subsequent to yielding, alloy specimens only rarely exhibited twinning on the stress-strain curve, regardless of temperature. Work hardening rates for all the alloys were greater than for pure cadmium, and tended to increase with increasing magnesium content. The exception was melt V, which had a higher rate of hardening than melts III and IV in spite of its lower magnesium content. It is believed that this was due to the introduction of non-metallic impurities during preparation of the melt.

The work hardening curves for the alloys containing up to 3.15 per cent magnesium tended to be parabolic, with decreasing rate for increasing strain until the onset of necking, as shown in Fig. 10 for melt III. Necking was pronounced

at room temperature, virtually to the same extent as for unalloyed cadmium. At lower temperatures, necking was terminated at temperatures which varied with alloy content, in conformance with the ductility transition curves to be discussed below. Qualitatively then the fracture process in these alloys resembled that for unalloyed cadmium.

For melts II and VII, the transition from elastic to plastic flow was very difficult to detect because of the extremely high work hardening rates in the plastic range. No yield points were observed at any temperature, nor were twin drops ever observed.

## 2. Strength vs. temperature and alloy content

In general, the yield strength and tensile strength of each of the alloys tended to increase with decreasing temperature, and decreasing grain size. True fracture stress data again were erratic with temperature, probably due to necking and the formation of intergranular cracks before fracture actually occurred.

However, there was a clear dependence of tensile strength on alloy content at room temperature,  $-77^{\circ}\text{C}$ ,  $-150^{\circ}\text{C}$  and  $-196^{\circ}\text{C}$ , as shown in Fig. 11 for specimens of similar grain sizes (with the one exception noted). The increase in strength is approximately linear up to 4.95 per cent magnesium, in spite of the

intervention of the ordering reaction near this composition. The limited data available for the 15.35 per cent alloy shows a tendency for the strength to level off, although the increase in strength is quite substantial. It is noteworthy that the data for  $-77^{\circ}\text{C}$ ,  $-150^{\circ}\text{C}$  and  $-196^{\circ}\text{C}$  fall on nearly the same curve, illustrating the tendency for strength to be constant with temperature at and below the transition range, for a given grain size. Therefore the alloys and pure cadmium behave quite similarly in this respect.

### 3. Fracture Behavior

Pertinent tensile data for each of the alloys are listed in Table 6. The alloys all showed a decrease in ductility, as measured by reduction in area and plastic elongation, with decreasing temperature. Ductility transition curves are presented in Figs. 12, 13 and 14 for melts III, IV and V respectively. Limited data available for the other alloys do not permit drawing transition curves. However, estimates of transition temperature can be made for most of the alloys, and are presented in Table 7 as temperatures for 50 per cent reduction in area and 20 per cent reduction in area.

Comparison of ductility data for pure cadmium and the alloys show certain definite trends:

- 1) The addition of magnesium to cadmium raises the ductile to "quasi-brittle" transition temperature.

- 2) For magnesium contents up to 3.15 per cent the ductility transition occurs well below room temperature. The 4.95 per cent alloy, melt II, exhibited only 39.9 per cent reduction in area at room temperature, compared to nearly 100 per cent for pure cadmium, indicating that the transition lies above room temperature for this alloy.
- 3) At  $196^{\circ}\text{C}$ , the lowest temperature for which comparisons are available, the ductility of all the alloys as measured by reduction in area is roughly the same, but about one-half that of pure cadmium. However, plastic elongation of melt II was far less than for the other alloys.
- 4) The effect of grain size on ductility was appreciable for melt II. This is to be expected in view of the relative brittleness of the alloy.

Although the plastic elongation of melt II was only a little over 1 per cent at  $-196^{\circ}\text{C}$ , the reduction in area was comparable to the other alloys. Melt VII, which one might expect to be extremely brittle because of its nearness to the composition for  $\text{MgCd}$ , showed plastic elongation and reduction in area very comparable to the other alloys tested at  $-196^{\circ}\text{C}$ .

#### 4. Microstructural Observations

The microstructures of deformed specimens of melts I, III, IV and V, containing up to 3.15 per cent magnesium were qualitatively similar to those of unalloyed cadmium. Basal

slip and twinning, as well as secondary basal slip within the twins, was observed at all temperatures. Kinking also was observed at all temperatures, including a specimen of melt IV tested at  $4.2^{\circ}\text{K}$ , see Fig. 15.

As with unalloyed cadmium, the grain structure near the fracture surface in necked specimens was almost obliterated. At lower temperatures the amount of slip and twinning was reduced, and clear observations of the fracture surface could be made. In all cases the fracture followed a saw-tooth pattern along the grain boundaries, exactly as for pure cadmium. Intergranular microcracks were noted in specimens deformed at  $-196^{\circ}\text{C}$  and interrupted just before fracture, as shown in Fig. 16b. Stopped cracks away from the fracture surface never were noted in fractured specimens of these alloys.

The non-basal deformation markings observed in unalloyed cadmium at  $-196^{\circ}\text{C}$  were noted to some extent in specimens of melts I, III, IV and V, but except for melt I to somewhat smaller extent. An example of these markings in melt IV is shown in Fig. 16a.

Microstructures of melts II and VII were much different than those for the other alloys and pure cadmium. Melt II exhibited almost no twinning, even up to the point of fracture, at any temperature. Those twins which did form, as identified

by repolishing techniques and polarized light, were small and very irregularly shaped, their width being a significant fraction of their length. A typical example is shown in Fig. 17 for a specimen tested at room temperature. The boundaries were neither straight nor smoothly curved, as are the usual lenticular twins in pure cadmium. Slip traces rarely were observed within these twins.

Basal slip traces also were seen, but to much less extent than in pure cadmium. Specimens interrupted just past the onset of plastic flow exhibited only a few widely spaced slip lines in a very small number of grains. Even fractured specimens did not exhibit slip lines in all grains. Several specimens, tested at  $-122^{\circ}\text{C}$  and  $-196^{\circ}\text{C}$ , also exhibited other markings never seen in pure cadmium or the other alloys. Figs. 18 to 20 show basal slip as the predominant set of traces, and what appears to be slip on a system at  $80^{\circ}$  to the basal plane. In fact, the overall appearance of the two sets of slip traces is quite similar to published photographs of basal and prismatic slip in polycrystalline magnesium<sup>38</sup> and magnesium-lithium alloys.<sup>19</sup> As in magnesium, the secondary traces have a crack-like non-crystallographic appearance at low magnifications. At higher magnifications, however, as in Figs 18b and 20, many additional traces appear, parallel to the darker markings. Repolishing removed the traces,

therefore seemingly ruling out cracks or twins as an alternate explanation for the non-basal traces. The markings were most often seen at grain corners and in grains adjoining the fracture surface, where presumably stress concentrations are the highest. This also is in agreement with observations on magnesium.<sup>38</sup> Transgranular fracture was noted in some of the grains which contained a large density of these markings as shown in Fig. 21b, but the fracture did not follow either the basal or non-basal traces. Stereographic analysis could not be employed to identify the traces because of the relatively fine grained material involved, but it will tentatively be assumed that the traces arise from  $\{10\bar{1}0\}$  prismatic slip.

Other markings noted on this alloy were formed at about  $35^\circ$  to the predominant basal slip traces, see Fig. 21a. Evidence of severe deformation often was noted adjacent to these markings. Repolishing did not remove the traces and it was not possible to determine whether they were due to fine cracks. However, the specimen shown in Fig. 21a exhibited transgranular fracture in a stepped pattern, one set of steps following these markings exactly. This is similar to the parting along narrow twins observed by Reed-Hill in magnesium.<sup>15</sup> Similar markings have been observed in polycrystalline cadmium tested in compression at  $-196^\circ\text{C}$ , as shown in Fig. 22. From the angle made by these traces with the basal plane, it is possible that



they arise from twinning on  $\{10\bar{1}3\}$ , which has been reported  
for magnesium.<sup>15</sup>

Very coarse, widely spaced slip traces were observed on all tensile specimens of melt VII, see Fig. 23, as well as on a bend specimen tested at room temperature. Fracture was observed to follow the slip traces in at least some grains at all temperatures. (The remainder of the fracture followed grain boundaries.) Bright cleavage facets were observed in all the grains which cleaved along the slip lines. A micrograph of a cleavage facet is shown in Fig. 24 for a specimen tested at  $-149^{\circ}\text{C}$ . Laue patterns taken perpendicular to the cleavage facet exhibited the six-fold symmetry characteristic of the basal plane, thereby establishing the cleavage plane as the basal plane. (Also, it may be concluded that slip occurred along the basal planes.) This appears to be the first observation of basal cleavage in cadmium or any cadmium base alloy yet reported.

#### 5. Compression Tests

In order to examine further the temperature dependence of deformation in cadmium-magnesium alloys, a few specimens of melts I, II, III and IV were tested in compression at room temperature,  $-77^{\circ}\text{C}$  and  $-196^{\circ}\text{C}$ . Also, a new alloy, containing 3.70 weight per cent magnesium and designated melt VIII, see Table 3, was tested at room temperature.

Increased resistance to deformation was noted with increasing alloy content and decreasing temperature as observed in tension. Microstructures of these specimens were examined at intervals of 1 to 3 per cent strain, followed by reloading after an elapsed time of the order of 30 minutes. Deformation markings were found to depend on temperature and alloy content for a given strain.

Melt I exhibited basal slip and twinning closely resembling the behavior of pure cadmium at room temperature and  $-196^{\circ}\text{C}$ . Traces that are believed to arise from non-basal slip were observed only at  $-196^{\circ}\text{C}$ , see Fig. 25, as for pure cadmium, Fig. 9b. Melts III and IV exhibited qualitatively the same deformation markings as pure cadmium except that considerably higher strains were necessary before slip and twin markings appeared in appreciable densities. This was particularly true at  $-196^{\circ}\text{C}$  where these alloys showed very little twinning until 8-10 per cent strain.

Melt II exhibited a few basal slip markings and twins at room temperature after 3 per cent strain, as shown in Fig. 26. These may be compared to deformation traces for a tensile specimen at room temperature, Fig. 17. Additional straining caused an increase in the number of grains with observable basal slip, but caused little additional twinning. At  $-196^{\circ}\text{C}$  still

fewer deformation markings were noted after equivalent strains.

Two very coarse grained specimens of melt VIII were tested in compression at room temperature. One specimen, VIII-1, kinked within a large grain at 11,100 psi. Microscopic examination, Fig. 27, revealed cracks along the slip plane, which is the basal plane. Faint markings at about  $90^\circ$  to the cracks can be seen in Fig. 27b. The origin of these traces is not known, although the angle of nearly  $90^\circ$  suggests prismatic slip as a possibility. Elsewhere on the same specimen, pyramidal  $\{11\bar{2}2\}$  slip was observed, as shown in Fig. 28. Pyramidal slip markings also were noted in the other specimen tested at room temperature. In each specimen they first appeared at a normal stress of about 11,000 psi.

## C. Twinning and Non-Basal Slip in Cadmium Single Crystals

### 1. Twinning in Tension

Single crystals oriented  $\chi_0 < 5^\circ$  were prepared from the two grades of cadmium and were tested at several temperatures in the range 23 to  $160^\circ\text{C}$ . None of the crystals appeared to be damaged prior to test, although very short twins were sometimes observed on the surface. Table 8 lists normal stresses at which the initial twin burst propagated for each crystal of 99.99<sup>+</sup> per cent cadmium. Similar data are shown in Table 9 for 99.95 per cent cadmium. Several interesting

features of the twinning behavior of the purer cadmium were noted. All but two of the eighteen specimens tested twinned at normal stresses of 1080 psi or less, corresponding to resolved shear stresses for twinning of less than  $400 \text{ g/mm}^2$ . Crystals Cd 14-1 and Cd-14-3, however, twinned at 2820 and 3270 psi respectively, corresponding to resolved shear stresses for twinning of about  $1050 \text{ g/mm}^2$ . Although both had been tested at elevated temperatures, this cannot be the responsible factor, since other crystals tested at the same temperatures twinned at very low stresses. If it is assumed, however, that twin nuclei were present in the crystals which twinned at low stresses, the results are easily explainable. It has been demonstrated for both zinc and cadmium that careless handling of crystals will cause twinning to occur at low stresses.<sup>4,10</sup> This is the reason for the wide scatter reported in the literature for critical stresses for twinning of these metals.<sup>10</sup> Cadmium crystals, moreover, were very susceptible to damage by the slightest contact of the polished surface with a foreign object. The very small twins produced by these contacts were sufficient to cause further twinning to progress at low stresses. The relative constancy of the stresses for twinning in these crystals suggests that a critical resolved shear stress law exists for the propagation of twin nuclei, in agreement with a suggestion by Thompson and Hingley.<sup>4</sup>

In view of the association of high twinning stresses in zinc with the appearance of pyramidal  $\{11\bar{2}2\}$  slip,<sup>10</sup> the two cadmium crystals which twinned at high stresses were examined very carefully for non-basal slip traces. Only in the case of Cd-14-3 were traces other than those due to basal slip or twinning observed. Fig. 29 shows traces inclined at about  $45^\circ$  to the basal slip traces, which are in turn nearly parallel to the specimen axis. Stereographic analysis of these traces was not possible, since they could be resolved only at very high magnifications, and did not extend very far around the specimens. Their general appearance, however, does not conform to  $\{11\bar{2}2\}$  slip. Attempts to repeat this experiment with other crystals were not successful.

The effect of temperature on twinning stresses, at least for crystals which presumably contain twin nuclei, appears to be negligible in the range 22 to  $160^\circ\text{C}$ . This behavior has previously been noted in zinc single crystals of similar orientation, tested in the range  $-77$  to  $100^\circ\text{C}$ . However, Thompson and Millard<sup>3</sup> reported that the resolved shear stress for twinning in 99.98 per cent cadmium was  $138 \text{ g/mm}^2$  at room temperature, but increased to  $295 \text{ g/mm}^2$  at  $-185^\circ\text{C}$ .

## 2. Non-Basal Slip in Compression

A compressive stress applied parallel to the basal plane of a cadmium single crystal cannot produce twinning or

appreciable basal slip.<sup>1</sup> Twinning is suppressed because the direction of the applied stress is opposite to the direction of the twinning shear, so that the crystal cannot relieve the applied stress by forming a twin. Basal slip is suppressed because the shear stress along the basal plane under these conditions is negligible. Therefore this orientation, tested in compression, offers the most favorable condition for the appearance of non-basal slip. The technique has previously been applied to zinc crystals,<sup>9</sup> resulting in the observation of pyramidal  $\{11\bar{2}2\} \langle 11\bar{2}3 \rangle$  slip, provided that  $\chi_0 < 3^\circ$ , and provided that kinking does not intervene. If kinking is suppressed, the crystal will deform by pyramidal slip until plastic buckling sets in.

A series of cadmium single crystals was prepared with  $\chi_0 < 5^\circ$ , great difficulty being encountered in approaching  $\chi_0 = 0^\circ$ .

Upon compressing these crystals, both at room temperature and at  $-196^\circ\text{C}$ , macroscopic kinking invariably occurred at normal stresses of the order of 900 to 1500 psi at room temperature, and about 1500 to 2000 psi at  $-196^\circ\text{C}$ . These stresses evidently were too low to allow non-basal slip systems to act, since clear non-basal traces could not be seen, except on one crystal which was taken to 5000 psi without kinking. In an attempt to overcome this problem, bicrystals and

tricrystals were prepared by growth from the melt. Each grain in these specimens tended to be oriented with the basal plane nearly parallel to the specimen axis. Application of compression to these specimens rarely resulted in kinking. Instead, no visible slip traces were noted until stresses of about 4000 psi were reached, when faint non-basal traces began to appear. With further straining the markings became more pronounced, as shown in Fig. 30. Also basal slip traces became visible. Stereographic analysis of the non-basal traces, with the aid of Laue patterns of the grains, confirmed that these were pyramidal  $\{11\bar{2}2\}$  slip traces. Continued stressing caused the traces to become more distinct and often traces of a second system were noted. In one case continued stressing caused a kink to form at a relatively high stress - 5720<sup>39</sup> psi. This type of kinking has been labelled "para" by Gilman to distinguish from the more usually encountered "ortho" kinks (at low stresses.)

At  $-196^{\circ}\text{C}$ , non-basal traces were first observed at about 8000 psi in compression tests on tricrystals. This is about 2 x the stress at which traces first appeared in tests at room temperature.

The critical resolved stress for the appearance of the first pyramidal slip traces in single crystals at  $-196^{\circ}\text{C}$  was

of the order of  $500 \text{ g/mm}^2$ , compared to a critical resolved shear stress for basal slip of  $85 \text{ g/mm}^2$  for material of similar purity tested by Thompson and Millard.<sup>3</sup>

Although no attempt was made to determine the slip direction by following the rotation of the specimen axis during deformation, observations of slip band intensities did not conflict with a choice of  $\langle \bar{1}1\bar{2}3 \rangle$ . The non-basal slip traces were strongest near the basal orientation and disappeared as the specimens were rotated  $90^\circ$  away from the basal plane. This rules out the choice of  $\langle \bar{1}1\bar{2}0 \rangle$  and  $\langle 10\bar{1}0 \rangle$ , since these directions lie in the basal plane. However, they are in agreement with the intensities which should be observed for  $\langle \bar{1}1\bar{2}3 \rangle$ .<sup>11</sup>

### 3. Non-Basal Slip in Bending

Since evidence of pyramidal slip was found in bicrystals and tricrystals tested in compression, while no such traces had been noted in tensile tests of single crystals, bending experiments were carried out to give further information on the role of direction of applied stress.

Single crystals, bicrystals and tricrystals were tested in four-point bending at room temperature and  $-196^\circ\text{C}$ . In the latter case the jig, with the crystal already in position, was immersed in liquid nitrogen, and the bending was applied after 5 minutes at temperature. Strains at the center,



or point of maximum bending, were measured with a micrometer. No provision was made for measuring stresses.

Pyramidal  $\{11\bar{2}2\}$  slip traces were observed on specimens tested at both temperatures. Examples are shown in Fig. 31 for a single crystal tested at room temperature, and Fig. 32 for a bicrystal tested at  $-196^{\circ}\text{C}$ . These traces were noted only on the compression side of the neutral axis. Twins, on the other hand, were noted primarily on the tensile side of the neutral axis, although they sometimes extended into the compression side.

There is an obvious difference in the appearance of the pyramidal slip traces at the two temperatures. At room temperature the traces are wavy, faint, and only in certain places concentrated in bands. At  $-196^{\circ}\text{C}$  the traces are always concentrated into bands, which bear a distinct resemblance to twins. Unlike twins, however, these bands are easily removed by repolishing. The bands resemble the non-basal traces noted above in polycrystalline cadmium and cadmium-magnesium alloys and it may tentatively be concluded that the latter bands arise from the same source. For both single crystals and polycrystals these bands appeared only at low temperatures, were easily removed by repolishing, and did not react under polarized light.

#### 4. Further Observations of Non-Basal Slip

A third method of studying the appearance of non-basal slip traces was simply to circumferentially scratch crystals of cadmium with a razor blade at several temperatures. Basal slip and twin traces were easily recognized, and in addition non-basal traces were observed on certain azimuths of these crystals. Fig. 33 shows the appearance of such traces adjacent to scratches applied at  $100^{\circ}\text{C}$ , room temperature, and  $-196^{\circ}\text{C}$ . The traces at  $100^{\circ}\text{C}$  and room temperature are qualitatively similar. They are wavy, faint and in some places collected into bands. The traces at  $-196^{\circ}\text{C}$ , on the other hand, are much clearer, relatively straight, and almost everywhere collected into bands. These observations are in accord with previous observations in bending and compression tests. A summary of slip traces observed on specimens tested by all 3 methods is presented in Table 10. In almost all cases for which complete analyses were carried out the same pair of planes was observed.

In addition, it was observed that the value of  $\lambda_0^*$  is not critical in determining whether non-basal slip will act, since  $\lambda_0$  ranged from  $2^{\circ}$  to  $15^{\circ}$  in these specimens.

Twin traces may increase or decrease in size upon annealing, while slip traces will be unaltered. In an effort to determine whether the observed traces might arise from twinning,

---

\* $\lambda_0$  is the angle between the specimen axis and the nearest close packed direction.

several scratched crystals were sealed in evacuated vycor capsules and heat treated at  $200^{\circ}\text{C}$  for several hours. No evidence of growth or contraction of these bands, either in a lateral or longitudinal direction, was noted.

#### IV DISCUSSION

##### A. Deformation of Polycrystalline Aggregates

Both the yield strength and work hardening coefficient for polycrystalline cadmium have been shown to be relatively insensitive to temperature in the range  $4.2^{\circ}\text{K}$  to room temperature. Similar results have been reported in the literature<sup>1,36</sup> for single crystals of cadmium. The critical resolved shear stress for basal glide at  $4^{\circ}\text{K}$  is barely twice that at room temperature.<sup>1</sup> Similarly the temperature dependence of the work hardening coefficient for most orientations of single crystals is nearly constant, at least between  $-50^{\circ}\text{C}$  and  $-196^{\circ}\text{C}$ .<sup>36</sup>

No drastic change in deformation modes appears in cadmium in this temperature range, although there is evidence of non-basal slip at sub-transition temperatures. Basal glide and twinning, as well as kinking and non-crystallographic tilt-boundary formation have been observed to persist to  $4.2^{\circ}\text{K}$  without much alteration in appearance.

The effect of grain size on the strength properties of cadmium is similar to other hexagonal metals, yield and fracture strengths being approximately proportional to  $d^{-1/2}$ . The large plastic deformation preceding fracture makes the latter result surprising, but similar behavior has been noted for magnesium which for sufficiently small grain sizes exhibits about 7 per cent elongation in the sub-transition region,<sup>34</sup> and for the ductile (60 per cent reduction in area) fracture of iron.<sup>35</sup>

Recrystallization was not observed during the straining of cadmium even at room temperature. However, substantial recovery of the flow stress was observed at room temperature, of the order of 30 per cent, compared to only 5 per cent recovery at  $-196^{\circ}\text{C}$ . This is in agreement with the reported temperature of  $-50^{\circ}\text{C}$  above which rapid recovery of cadmium single crystals is observed.<sup>36</sup> Although this factor probably contributes to the reduced ductility at lower temperatures, a detailed explanation of the ductility transition is not yet possible. However, the high residual ductility at low temperatures can be rationalized, for which see section IV C.

The addition of magnesium to cadmium causes an approximately linear increase in tensile strength with weight per cent magnesium added, at least to 5 per cent magnesium.

Data for the tensile strength of magnesium base alloys reported by Raynor<sup>40</sup> reveal that 5 per cent cadmium (1 atomic per cent) added to magnesium in the "soft" condition raises the tensile strength by 15 per cent. Hauser, et al<sup>19</sup> report that adding 12.7 atomic per cent cadmium raises the true fracture stress of magnesium by about 50 per cent. The latter result is in accord with the effect of adding magnesium to cadmium, as shown in Fig. 11. This is to be expected for two metals of the same crystal structure and valence, since the atomic size factor is expected to be the controlling factor in solid solution hardening.

The ductility of cadmium is reduced by the addition of magnesium, but the effect of cadmium on magnesium is not clear. Raynor<sup>40</sup> reports that cadmium increases the ductility of magnesium, while Hauser et al<sup>19</sup> report that the ductility of magnesium is reduced (at -196°C). Since solutes generally reduce the ductility of the solvent metal, the behavior of cadmium-base alloys is not unusual.

Although the addition of magnesium to cadmium in amounts up to 3.15 per cent does not affect the fracture mode, the ductile to "quasi-brittle" transition temperature is raised. The effects observed in connection with the deformation and fracture of the alloys can best be explained by the fact that

the yield stress of cadmium is raised far more than the fracture stress at low temperatures. Coupled with the higher rates of work hardening in the alloys, this causes the flow curve to be terminated at lower strains for the same temperatures.

The fracture mode was changed only for the two alloys of highest magnesium content. Melt II had an extremely high rate of work hardening and low ductility particularly in terms of plastic elongation. This behavior may be attributed to the sharp decrease in the amount of strain available from twinning, as well as the presumed introduction of prismatic slip. Prismatic slip has been associated with extremely high rates of work hardening, as for example in rhenium, titanium and beryllium.<sup>41</sup> Another factor is the introduction of the ordering reaction, which might tend to increase the work hardening rate.<sup>42</sup>

The relatively small amount of twinning in this alloy can most probably be attributed to the axial ratio of about 1.77 in the disordered state. The twinning shear, or shear at unit distance from the twinning plane under the action of an applied stress, is given by<sup>1</sup>

$$s = \frac{\left(\frac{c}{a}\right)^2 - 3}{\sqrt{3} \cdot \frac{c}{a}} \quad (2)$$

For cadmium and zinc, with  $c/a > \sqrt{3}$ ,  $S$  is positive, while for all other hexagonal metals it is negative.

A necessary condition for twinning is that the shear stress resolved on the twinning plane and in the twinning direction shall have the same sense as the twinning shear. It is generally observed that twin width is inversely proportional to the twinning shear<sup>16</sup>. For an axial ratio of 1.732 the shear is zero. For such a material the application of a shear stress should not result in twin formation, since there is no strain energy relief. Therefore, as suggested by Barrett<sup>18</sup> in a discussion of twinning in the hexagonal metals, a material with an axial ratio of 1.732 should not twin. The present results support this reasoning. Additional support is provided by work of Aaronson and co-workers.<sup>43</sup> Diffusion couples made by welding pure magnesium to pure cadmium exhibit twinning throughout the diffusion zone, with the twin appearance depending on composition. At compositions approaching that for which the  $c/a$  ratio is 1.732, there is almost a complete absence of twinning.

Attempts were made to verify this phenomenon by preparing new alloys with axial ratios almost identical to 1.732. These alloys were so brittle, however, that even swaging just below the melting point was unsuccessful in avoiding cracking.

One might ascribe this to the nearness of the desired composition to the superlattice composition  $\text{MgCd}_3$ , except that Melt VII, with 45.6 atomic per cent magnesium, was not swaged without any difficulty. The latter composition is very close to the superlattice  $\text{MgCd}$ . In any case all swaging was carried out near  $300^\circ\text{C}$ , well above the ordering temperatures of these alloys. It seems likely, therefore, that the axial ratio is the critical factor influencing the ductility of such alloys.

Although zinc cleaves completely at all temperatures below its transition temperature, the appearance of basal cleavage in specimens of melt VII was not sufficient to cause complete fracture of the specimen even at  $-196^\circ\text{C}$ . Cleavage facets were revealed at room temperature and all lower test temperatures. The cleavage facets exhibited river patterns, shown in Fig. 24, as in zinc, but no other identifiable markings. Basal slip lines on the specimen surfaces were very coarse and relatively widely spaced, in contrast to the narrow closely spaced slip lines of pure cadmium and the other alloys. This is to be expected for an ordered alloy, since the initial deformation due to slip destroys the local order and makes subsequent slip on the same planes more likely than on new planes.

Basal cleavage was observed also in one other case, a 3.70 per cent magnesium alloy. A coarse grained specimen



was compressed at room temperature, and cracking along the slip plane was noted in a region containing multiple kinks, as shown in Fig. 27. One of the cracks extended completely through the specimen. Similar cracks have been noted in zinc single crystals tested in compression, and Stroh<sup>44</sup> has discussed the dislocation interactions leading to crack formation under these conditions. When a slip band crosses a tilt boundary, the sides of the boundary are displaced, and a crack is produced along the slip plane.

Attempts were made to widen the largest observed crack by inserting a pin after the specimen was cooled in liquid nitrogen. When this failed a razor blade was inserted in the crack under the same conditions, again with no success. This indicates the extreme resistance to propagation of cleavage cracks in these materials.

#### B. The Ductility Transition in Hexagonal Metals

While the theory of brittle fracture in polycrystalline body centered cubic metals has been fairly extensively developed,<sup>32,45,46</sup> the causes of brittle fracture in hexagonal close packed metals are less well understood. Six hexagonal metals: cadmium, zinc, magnesium titanium, zirconium and beryllium are listed in order of decreasing axial ratio in Table 11.

Of these, cadmium zinc and magnesium undergo a sharp drop in ductility over a relatively narrow temperature range, while no abrupt ductility transition occurs for zirconium or titanium.<sup>12</sup> Beryllium is well known to be brittle under most conditions<sup>46</sup> except at elevated temperatures.

Zinc and beryllium are the only hexagonal metals in which crystallographic cleavage is observed. The "brittle" failure of cadmium as shown in these experiments, is always intergranular, while the brittle fracture of magnesium is a mixture of transgranular and intergranular failure. For both metals the plastic deformation preceding fracture is appreciable.

Of all these metals only zinc may be considered to undergo a true ductile - brittle transition, as the fracture mode changes from shear to cleavage with decreasing temperature. Brittleness in magnesium has been ascribed to a transition from hot working, accompanied by recrystallization, to cold working in the ductility transition range.<sup>37</sup> The brittleness of beryllium often has been ascribed to the presence of impurities such as BeO,<sup>47</sup> but the problem still is not well understood. In cadmium, recrystallization of deformed specimens was not observed even at room temperature, over 100°C above the temperature where ductility begins to fall off.

However, no transition to cleavage failure is involved, even at  $4.2^{\circ}\text{K}$ , regardless of grain size, or at  $-196^{\circ}\text{C}$ , regardless of grain size, strain rate, or triaxiality of stressing (due to presence of a circumferential notch).

Differences in axial ratio obviously cannot explain the wide variation in fracture modes among these metals, since zinc, with the second highest axial ratio of the six, and beryllium, with the lowest, both exhibit cleavage while the other metals do not. The factor of axial ratio also was eliminated by the results on fracture of cadmium-magnesium alloys.

The high ductility of cadmium persisting down to the lowest test temperature may be thought unusual in view of Taylor's argument that plastic deformation cannot occur in polycrystalline aggregates unless each grain can undertake at least five independent mechanisms of deformation.<sup>48</sup> Basal slip can provide only two independent mechanisms, and twinning can provide six additional mechanisms. However, the deformation that can be obtained by twinning is severely limited; the maximum elongation that can be obtained upon complete twinning of a single crystal of the optimum orientation is only about 7 per cent.<sup>1</sup> Since the grains of a polycrystalline aggregate are randomly oriented, and are rarely converted entirely to a twinned orientation (at least at low temperature), the total

strain obtained as a result of twinning should be appreciably less than 7 per cent.<sup>19</sup> Slip within the twins also occurs of course, but constraints at the twin boundaries may be expected to limit this contribution.<sup>19</sup> Assuming a maximum contribution from twinning, two additional independent mechanisms of deformation must be induced in order for the grains to deform to any arbitrary shape. Without these additional modes, brittle fracture may be expected to occur as a consequence of dislocation pile-ups at grain boundaries. Under these conditions the brittle fracture strength is given by<sup>32,45,46</sup>

$$\sigma_F = \sigma_0 + kd^{-1/2} \quad (1)$$

where  $\sigma_0$  is a "frictional" stress on a dislocation array, and  $k$  is a constant depending on the average distance and orientation of the crack nucleus from the head of the dislocation array.

While cadmium was found to obey a law of this sort below the transition range (see Fig. 6 for data at  $-196^\circ\text{C}$ , with  $\sigma_0 = 0$ ) the fracture was not truly brittle. The large amount of plastic deformation preceding fracture suggests that additional deformation modes must operate at sub-transition temperatures. The relatively small amount of pyramidal slip observed at  $-196^\circ\text{C}$  would not be sufficient to provide the additional deformation necessary. However, kinking about an axis normal to the basal slip direction, as well as

accomodation kinking parallel to twins, have been observed at low temperatures, along with low angle non-crystallographic tilt boundaries. Therefore, the contribution of several minor modes of deformation evidently is sufficient to cause the observed elongations at  $-196^{\circ}\text{C}$  and  $-269^{\circ}\text{C}$ .

Since the fracture at sub-transition temperatures is not truly brittle, one must examine the applicability of equation (1) to the fracture of cadmium. The fact that this equation is even approximately obeyed suggests that dislocation pile-ups do occur and ultimately cause failure.<sup>35</sup> Obstacles to dislocation movement are most likely to be grain boundaries or twin boundaries. In the case of zinc, both type of boundary evidently are effective, fracture having been observed to originate under conditions of dislocation pile-ups:

- a) At a grain boundary, causing a crack to form along the pile-up.<sup>49</sup>
- b) At twin intersections, with the crack propagating along the line of twin intersections, on the basal planes within the twins.<sup>50</sup>
- c) At kink bands.<sup>51</sup>

Occasionally also a single crystal which cleaves through method b) has an accompanying step when cleavage occurs on the basal plane of the matrix.<sup>50</sup>

In cadmium, however, neither twin intersections nor any other phenomena ever have been noted to induce cleavage failure. Single crystals of cadmium oriented  $\chi_0 < 5^\circ$  necked down to a flat ribbon even at  $-196^\circ\text{C}$ , which is observed for zinc crystals of similar orientation at elevated temperatures only.

It appears likely then that twin boundaries in cadmium are relatively open to the passage of slip dislocations, whereas in zinc the twin boundaries are opaque. Another indication of the relative ineffectiveness of twin boundaries in cadmium is the constant work hardening rate between yielding and the onset of necking, at and below the transition range from ductile to quasi-brittle failure. Thus once dislocations begin to move along the basal planes in cadmium, they are unimpeded by the twins, which form in great numbers, or at best, hardening due to twins is offset by the strain provided by the twins themselves and the new basal slip system within the twins. In fact, the twins will themselves re-twin without giving rise to high enough stresses to cause failure.

### C. Cleavage in Metals

<sup>52</sup>  
Gilman has reviewed the criteria suggested for predicting or rationalizing the observed cleavage planes of crystals. A purely geometric criterion states that the cleavage plane

of a crystal is its most closely packed plane. There is also the criterion that the cleavage plane is the plane which cuts a minimum number of chemical bonds per unit of area. Finally there is the criterion that the plane of minimum surface energy should be the cleavage plane. Leaving aside the question of chemical bonds, the geometrical and minimum surface energy criteria both suggest that the basal plane should be the cleavage plane in cadmium. The cleavages in certain alloy specimens confirm this, but do not explain why pure cadmium does not cleave.

Gilman proposes a mechanical criterion for the cleavage plane, which states that the observed cleavage plane should be the one which requires the least force to propagate a cleavage crack along it. The material constants that determine this force are shown to be the elastic modulus  $E$  and the true elastic surface energy  $\gamma$ , through a relation of the form  $F = \text{const.} \sqrt{\gamma E}$ .

Little is known concerning the anisotropy of surface energies in metals. Gilman has provided a means of estimating surface energy as follows:

Assume that the attractive stress  $\sigma (y)$  between two surfaces is given by

$$\sigma (y) = \sigma_0 \sin \frac{\pi y}{a} \quad 0 \leq y \leq a \quad (3)$$

Where  $a$  is the "range" of the elastic forces.

For small displacements  $\sigma(y)$  should obey Hooke's law, and

$$\sin \frac{\pi y}{a} \sim \frac{\pi y}{a} \quad (4)$$

This leads to the relation

$$\sigma = E \left( -\frac{y}{y_0} \right) = \sigma_0 \frac{\pi y}{a} \quad y \ll a \quad (5)$$

where  $y_0$  is the equilibrium lattice constant perpendicular to the plane. With  $\sigma_0$  determined, the attractive stress becomes:

$$\sigma(y) = \frac{E a'}{\pi y_0} \sin \frac{\pi y}{a} \quad (6)$$

Since the surface energy is one-half the energy required to separate two surfaces:

$$\gamma = \frac{1}{2} \int_0^{a'} \sigma(y) dy = \frac{E}{y_0} \left( \frac{a'}{\pi} \right)^2 \quad (7)$$

This equation indicates that cleavage will occur on those planes for which  $E$  is a minimum, the interatomic distance  $a'$  is a minimum, and the interplanar distance  $y_0$  is a maximum. Using values for  $E$ ,  $y_0$  and  $a'$  obtained from Barrett<sup>5</sup> for the basal plane of cadmium, one obtains  $\gamma = 224 \text{ ergs/cm}^2$ . This compares with a value of  $254 \text{ ergs/cm}^2$  calculated for zinc using equivalent quantities. The surface energies calculated for the prism planes are several times higher for both metals, suggesting that the basal plane should be the preferred cleavage plane. Gilman, using a higher value of  $E$ , found a value



for  $\gamma$  of 400 ergs/cm<sup>2</sup>. The true surface energy of zinc is generally considered to be about 1000 ergs/cm<sup>2</sup>. Therefore the present calculation for cadmium is probably correct to within an order of magnitude.

On the basis of these considerations, cadmium, with low values of surface energy,  $\gamma$ , and elastic modulus,  $E$ , should cleave as easily as zinc if not more so.

It is necessary, however, to take into account the energy absorption during cleavage. In ideal cleavage, the work that is done by the applied force  $F$  is all converted into true surface energy. In most real crystals however, plastic deformation, anelastic and electrical effects and the formation of cleavage steps all absorb some of the energy. An effective surface energy  $\gamma_c$ , which is the sum of the true surface energy  $\gamma$  and the energies of other absorbing processes must be used instead.

Plastic flow during cleavage will probably make the largest contribution to  $\gamma_c$ , and crystals that contain boundaries or large numbers of dislocations will tend to absorb still larger amounts of plastic energy. Under such conditions  $\gamma_c$  can attain values as high as  $10^5 - 10^8$  ergs.<sup>52</sup>

The Griffith condition<sup>53</sup> for crack propagation in the

cylindrical specimens used in this investigation may be approximated by:

$$\sigma_F = \left( \frac{\gamma_c d}{a} \right)^{1/2} \quad (8)$$

with  $c$  taken as the average grain diameter, and  $a$  a constant of the order of magnitude of unity. This equation was applied to the fracture data for polycrystalline cadmium shown in Fig. 6. The effective surface energy  $\gamma_c$  under these conditions was calculated to be  $3.99 \times 10^5$  ergs/cm<sup>2</sup>, or about three orders of magnitude greater than the calculated "true" surface energy. Similar calculations were performed for the fracture of zinc and of magnesium, as reported by several investigators and summarized in Table 12. The ratio  $\frac{\gamma_c}{\gamma}$  is highest for cadmium, although for both zinc and magnesium the observed surface energy is at least an order of magnitude higher than the calculated value.

<sup>35</sup>Petch has discussed ductile fracture in iron, which follows a  $d^{-1/2}$  law with the same slope as for cleavage fracture and suggests that the fracture stress (corrected for necking) is still determined by the condition for crack formation ahead of a dislocation array. However, this will not be the first crack that forms, but some subsequent one. The stress required for the dislocation array that produces this subsequent crack should not be much different from that

required for the initial crack. Therefore, the stress due to a dislocation array should be about the same as would have produced cleavage, if cleavage were possible at that temperature. The crack that eventually will cause fracture is expected to form early in the test, but further extension of the specimen is required until the work required for its extension can come from the stored elastic energy. The fracture will then become a fast one, and the condition for its propagation will resemble that for a Griffith crack, with plastic energy added to the surface energy.<sup>35</sup> However, for cadmium the first cracks are not noted until just prior to the onset of necking, suggesting that the imposition of triaxial stresses is necessary to make the cracks open to visible dimensions.

<sup>54</sup>Stroh has discussed Petch's theory, and points out that the intercept  $\sigma_0$  in equation 1 will be affected by all the factors determining the flow stress of a work hardened material. However, no theoretical treatment of  $\sigma_0$  in the ductile case has been given. The problem becomes still more difficult when dealing with materials such as zinc and cadmium where  $\sigma_0 = 0$ .<sup>46</sup> Cottrell, however, states that glide planes in close packed metal crystals have low Peierls-Nabarro forces, which may account for  $\sigma_0 = 0$ .

It seems clear that any material which has a low yield

stress which is not markedly influenced by temperature or by impurities (dislocation locking), as is the case for cadmium, will not be likely to undergo brittle fracture. The yield stress  $\tau_y$  is low even to 4.2°K, and is not strain rate sensitive at low temperatures. Similarly Churchman<sup>41</sup> has pointed out that despite the high rate of work hardening of rhodium, the cleavage stress is not reached because dislocation locking does not occur.

By adding magnesium to cadmium,  $\tau_y$  is raised considerably, while the effect on  $\gamma_c$  is uncertain. The fact that the 15.35 per cent alloy did exhibit cleavage over a wide temperature range suggests that  $\gamma_c$  actually was lowered considerably, since the other alloys had comparable yield stresses without cleavage being induced. The cleavage induced in the 3.70 per cent magnesium alloy is excluded from this discussion because of the influence of the dislocation arrays in the kink bands.

It seems evident that the high ductility of cadmium at low temperatures is a consequence of several factors, foremost among them being the magnitude of the yield stress and the persistence of several minor deformation modes. Since the yield stress is neither temperature nor strain rate sensitive, neither of these variables is very helpful in reducing ductility. Also, the low value of the yield stress and

the absence of a yield point insures that dislocation pile-ups are easily relieved by localized plastic flow. Therefore when dislocations begin to pile up at grain boundaries on other obstacles in the early stages of plastic deformation, yielding occurs in the surrounding matrix. This limits the size of pile-ups that can form, and stress concentrations are not large. Subsequent deformation work hardens the matrix to the extent that pile-ups can attain greater lengths without stress relaxation occurring. A crack will then be nucleated, and grow to macroscopic proportions along a grain boundary. Further deformation results in rapid propagation of the crack, and the specimen breaks.

#### D. Non-Basal Slip

For zinc, cadmium and magnesium, the appearance of pyramidal slip has been restricted to single crystals oriented with the basal plane nearly parallel to the stress axis. This orientation is one for which the applied stress resolved parallel to the basal plane is a minimum, thus effectively suppressing basal slip and allowing the pyramidal planes to operate.

Bell and Cahn<sup>10</sup> reported pyramidal slip occurred in zinc crystals tested in tension, and were able to obtain micrographs showing slip on two  $\{11\bar{2}2\}$  planes. However, the traces were clearly seen only on a small number of crystals. It was

suggested that when slip on pyramidal and basal planes occurred simultaneously, twinning was initiated. Basal slip traces then appeared in clusters or "bunches".

Gilman<sup>9</sup> observed pyramidal slip on zinc crystals oriented  $\chi_0 \leq 5^\circ$  tested in compression. The maximum load supported by specimens could be associated with the onset of "plastic buckling" of the crystal. As confirmed by preliminary work on zinc for this project, the stress for buckling is inversely proportional to the specimen length, and the work hardening depends strongly on the orientation factor  $\lambda_0$  and on the testing temperature.

Tensile tests performed by Gilman<sup>9</sup> on specimens taken from the same crystals that were used for compression tests showed only elastic deformation up to loads that produced twinning ( $3.7 \text{ kg/mm}^2$ ). These stresses were considerably higher than the  $0.2$  to  $0.3 \text{ kg/mm}^2$  required to start plastic deformation in compression. Similarly, in tests carried out on zinc crystals for this project, no pyramidal traces were seen on specimens carried up to the point of twinning. However, Price<sup>54</sup> recently demonstrated that  $\{11\bar{2}2\} \langle 11\bar{2}3 \rangle$  glide operates in basal oriented platelets of zinc tested in tension. Also, several investigations have observed markings on cleavage surfaces which were labeled kink bands, but were later

identified by Rosenbaum<sup>56</sup> as pyramidal  $\{11\bar{2}2\}$  traces. During the present investigation a number of observations of pyramidal slip traces corresponded closely with the observations of Gilman<sup>9</sup> and Rosenbaum<sup>56</sup> on zinc.

Traces were most prominent at  $-196^{\circ}\text{C}$ , and virtually identical in appearance at room temperature and  $100^{\circ}\text{C}$ . Gilman<sup>9</sup> also observed more prominent bands at lower temperatures. The traces were orientation dependent, being most prominent when bending was parallel to  $(0001)$ , as observed by Rosenbaum<sup>56</sup> for zinc, or when scratches were made on basal surfaces. The traces were unevenly spaced and wavy at room temperature and  $100^{\circ}\text{C}$ , but relatively straight at  $-196^{\circ}\text{C}$ . They often were accentuated at grain boundaries, scratches, and other inhomogeneities. In compression tests, they often were associated with bunched basal slip, an example of which is shown in Fig. 30,<sup>10</sup> as observed by Bell and Cahn in tension tests.

The traces usually were found on either one or two  $\{11\bar{2}2\}$ , in contrast to zinc which exhibits as many as four different systems.<sup>9</sup> In general, rather severe straining was required for the traces to stand out, although they first were visible at rather low stress, of the order of 2000 psi in compression tests at room temperature.

In cadmium, as in zinc, kinking often competes with

pyramidal slip as a deformation process in compression. However, two types of kinking have been observed:

- a) That occurring at extremely low stresses in which the basal planes gradually bend over into a single macroscopic kink.
- b) That occurring at relatively high stresses in which multiple kinks form suddenly in the gage section with a loud report, as in twinning.

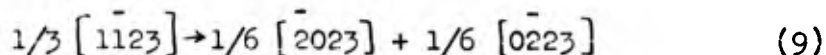
With kinking of type a), pyramidal slip is rarely seen in zinc or in cadmium. With kinking of type b), pyramidal slip traces are seen, no doubt due to the high stress levels which can be obtained prior to the introduction of kinking.

It seems likely that the difficulty in observing pyramidal slip in cadmium arises from the competition of twinning and kinking in tension and compression tests respectively. Once either of these mechanisms begins to operate pyramidal slip is suppressed as a stress-relief mechanism. When Bell and Cahn prevented twinning from occurring until very high stress levels, pyramidal slip became prominent. Similarly, the zinc platelets tested by Price<sup>55</sup> in an electron microscope exhibited twinning only at very high stress levels, allowing pyramidal slip to operate prior to the formation of the first twin.

Price<sup>55</sup> proposed that the  $\{11\bar{2}2\}$  planes may be favored over other pyramidal planes (e.g.  $\{10\bar{1}1\}$ ) because the  $\langle 11\bar{2}3 \rangle$



dislocations can lower their energy by splitting into partials on the former in a reaction of the type:



These dislocations are able to glide easily from one pyramidal plane to another, and it was concluded that they are of screw character.

The fact that pyramidal slip is observed in cadmium only when extraordinary precautions are taken to suppress kinking and twinning indicates that it is not a major deformation mode. Moreover, the onset of pyramidal slip appears to have no effect on subsequent fracture behavior, except insofar as pyramidal dislocations may contribute to hardening of the lattice.

## V SUMMARY AND CONCLUSIONS

The results obtained in this study of deformation and fracture in cadmium and cadmium-magnesium alloys can be summarized as follows:

1. The yield stress, flow stresses for arbitrary small strains and the average coefficient of work hardening for cadmium polycrystals were found to be relatively insensitive to temperature in the range from room temperature to 4.2°K.
2. The tensile strength of cadmium was strongly temperature

dependent but relatively independent of grain size between room temperature and  $-175^{\circ}\text{C}$ . Below  $-175^{\circ}\text{C}$ , the tensile strength was dependent on grain size, but not on temperature, for a given grain size.

3. The true fracture stress at  $-196^{\circ}\text{C}$  was found to depend on grain size through the relation:  $\sigma_F = \sigma_0 + kd^{-1/2}$ , with  $\sigma_0 = 0$  and  $k = 3050$  (psi) in  $^{1/2}$ . A similar relation was found for yield stress at  $-196^{\circ}\text{C}$ , with  $\sigma_0 = 0$  and  $k = 560$  (psi) in  $^{1/2}$ . In the c.g.s. system the values of  $k$  were  $3.34 \times 10^8$  and  $0.61 \times 10^8$  (dynes/cm<sup>2</sup>) cm $^{1/2}$  respectively.

4. Cadmium undergoes a ductile to "quasi-brittle" transition at about  $-155^{\circ}\text{C}$  for a crosshead rate of 0.01 in./in./min. The transition temperature did not depend on grain size or on minor differences in purity. The minimum ductility of about 15 per cent reduction in area was reached near  $-196^{\circ}\text{C}$ , and persisted at  $-269^{\circ}\text{C}$ .

5. The decrease in ductility in the transition range did not involve recrystallization during deformation. No major changes in the mechanism of plastic deformation were noted, although there was evidence of the introduction of non-basal slip at sub-transition temperatures. The cause of the rapid drop in ductility with decreasing temperature is not known, although reduced recovery may be a factor. Fracture at low temperatures always occurred along the grain boundaries..

6. The ductility at  $-196^{\circ}\text{C}$  could not be reduced appreciably by employing faster strain rates, testing specimens with a circumferential notch, or by adding magnesium up to 3.15 weight per cent, even for the coarsest grain sizes used.

7. The addition of magnesium to cadmium produced a large increase in yield strength at all temperatures. Tensile strengths and fracture strengths throughout the entire temperature range also were raised, but not as much as the yield strengths, particularly at lower temperatures. The increase in tensile strength was approximately proportional to the weight per cent of magnesium added. Although slip and twinning occurred at higher stress levels, there was no change in deformation modes for magnesium contents up to 3.15 per cent, in spite of a significant decrease in the axial ratio.

8. Transcrystalline fractures were achieved in some grains of a 4.95 per cent magnesium alloy. This alloy, with an axial ratio in the disordered state of about 1.77, exhibited much less twinning than pure cadmium or any of the other alloys. This was attributed to the approach of the axial ratio to 1.732, for which no twinning is to be expected on the basis of calculations of twinning shear. Attempts to hot work alloys with  $c/a$  ratio near 1.732 were unsuccessful, even though the alloys were in the disordered condition. These results supported the hypothesis that brittleness in these alloys results

from a lack of ability to deform appreciably by twinning, rather than from superlattice formation.

9. Basal cleavages were achieved in two alloys, by testing in tension, bending and compression. These appear to be the first reported cleavages in cadmium-base materials. The observation of cleavage cracks in the vicinity of kink bands for the 3.70 per cent magnesium alloys appears to be only the second reported for the hexagonal metals, and extends the applicability of Stroh's analysis<sup>44</sup> of the origins of cracks at tilt boundaries.

10. Pyramidal  $\{11\bar{2}2\}$  slip was found to operate in cadmium single crystals oriented with  $\chi_0 < 5^\circ$ . Traces of these planes were observed in bending and compression tests at room temperature,  $-196^\circ\text{C}$  and  $100^\circ\text{C}$ . At  $-196^\circ\text{C}$  the traces were straight and sharply defined, while at high temperatures they were wavy and indistinct. The critical resolved shear stress for the appearance of pyramidal slip in single crystals is estimated to be about  $500 \text{ g/mm}^2$  at  $-196^\circ\text{C}$ . Kinking and twinning were postulated to be competitive processes for stress relief, which often cause pyramidal slip to be suppressed.

The fracture behavior of cadmium was analyzed in terms of the deformation modes observed at various temperatures and in terms of several proposed dislocation models for

fracture.<sup>35,45,46</sup> The test results were found to agree in many details with Petch's analysis<sup>35</sup> of ductile fracture in iron, particularly in the dependence of fracture stress on  $d^{-1/2}$ . It was concluded that "quasi-brittle" fracture in cadmium is a consequence of the low yield stress and absence of dislocation locking, which permit incipient dislocation pile ups to disperse by plastic deformation in the matrix.

An estimate of the effective surface energy for fracture was obtained using a modified Griffith<sup>53</sup> equation from fracture data at  $-196^{\circ}\text{C}$ , and was shown to be about  $10^3$  times a calculated "true" surface energy for elastic cleavage. This difference between effective and "true" surface energies was found to be considerably higher than for zinc or magnesium, which exhibit much less plastic deformation prior to fracture.

## VI SUGGESTIONS FOR FUTURE WORK

In order for cleavage to be induced in cadmium, it seems to be necessary to simultaneously lower the surface energy and raise the yield stress. Recent work showing the effectiveness of mercury in embrittling otherwise ductile metals indicates that the effect is due to the low energy of a solid metal - liquid metal interface.<sup>57</sup> Therefore it would be advisable

to experiment with mercury and possibly other liquid metals to attempt to induce cleavage in cadmium. Initial work should be carried out on single crystals to eliminate complicating effects of grain boundary embrittlement.

Observations of  $\{11\bar{2}2\}$  pyramidal slip in cadmium single crystals should be continued to obtain additional information concerning the role of compression in favoring the appearance of traces on this system. Although this is highly unusual behavior for a slip system, the experimental evidence shows little likelihood that these markings are minute twins rather than slip traces.

It would be desirable to study further the fracture behavior of alloys with  $c/a$  ratio near 1.732. Much of the difficulty in obtaining useful information on slip in cadmium is the ever-present intervention of twinning which acts as a stress relief mechanism while obscuring the microstructure. Positive identification of the slip traces which resemble prismatic slip in alloys with this  $c/a$  ratio is desirable.

## VII ACKNOWLEDGMENTS

The author is indebted to Mr. Leo Boyajian for constructing most of the equipment necessary for this investigation,

and to Mr. Melvin Bernstein for assistance in carrying out many experiments. The author also wishes to thank Mr. Edward Aqua for carrying out electrical resistivity measurements on an ordered alloy. This investigation was carried out under the sponsorship of Prof. M. Gensamer.

The research performed in this investigation was supported by the Air Force Office of Scientific Research, under Contract AF 49(638)-408.

## BIBLIOGRAPHY

1. E. Schmid and W. Boas, Plasticity of Crystals, F.A. Hughes, London, 1950.
2. E.N. da C Andrade and R. Roscoe, Proc. Phys. Soc., v. 49, 1937, p. 152.
3. N. Thompson and D.J. Millard, Phil. Mag., v. 43, 1952, p. 421.
4. N. Thompson and M. Hingley, Acta Met., v. 3, 1955, p. 289.
5. C.S. Barrett, Structure of Metals, McGraw Hill, New York, 1952.
6. A.F. Brown, Advances in Physics, v. 1, 1953, p. 427.
7. J.H. Wernick and E.E. Thomas, AIME Trans., v. 218, 1960, p. 769.
8. P.B. Price, Bull. Am. Phys. Soc., Series II, v. 6, 1961, p. 76.
9. J.J. Gilman, AIME Trans., v. 203, 1955, p. 206.
10. R.L. Bell and R.W. Cahn, Proc. Roy. Soc., v. 239A, 1957, p. 494.
11. R.E. Reed-Hill and W.D. Robertson, AIME Trans., v. 212, 1958, p. 256.
12. A.W. Magnusson and W.M. Baldwin, Jr., J. Mech. Phys. Solids, v. 5, 1957, p. 172.
13. J.J. Gilman, AIME Trans., v. 206, 1956, p. 1326.
14. R.E. Reed-Hill and W.D. Robertson, AIME Trans., v. 209, 1957, p. 496.
15. R.E. Reed-Hill and W.D. Robertson, Acta Met., v. 5, 1957, p. 728.
16. F.D. Rosi, C.A. Dube and H. Alexander, AIME Trans., v. 197, 1953, p. 257.



17. A.R. Chaudhuri, H.C. Chang and N.J. Grant, AIME Trans., v. 203, 1955, p. 682.
18. C.S. Barrett, Cold Working of Metals, ASM, Cleveland, 1949, p. 65.
19. F.E. Hauser, R.R. Landon and J.E. Dorn, ASM Trans., v. 50, 1958, p. 856.
20. A.H. Cottrell and D.F. Gibbons, Nature, v. 162, 1948, p. 488.
21. E.O. Hall, Twinning and Diffusionless Transformations, **Butterworths**, London, 1956.
22. A.T. Churchman, Proc. Roy. Soc., v. 226A, 1954, p. 216.
23. Metals Handbook, ASM, Cleveland, 1948, p. 21.
24. D.A. Edwards, W.E. Wallace and R.S. Craig, J. Am. Chem. Soc., v. 74, 1952, p. 5256.
25. W. Hume-Rothery and G.V. Raynor, Proc. Roy. Soc., v. 174A, 1940, p. 471.
26. J.J. Gilman and V.J. De Carlo, AIME Trans., v. 206, 1956, p. 511.
27. D.F. Phillips and N. Thompson, Proc. Phys. Soc., v. 63B, 1950, p. 839.
28. E.N. da C Andrade and R.F. Randall, Proc. Phys. Soc., v. 65B, 1952, p. 445.
29. L.C. Weiner and M. Gensamer, J. Inst. Met., v. 85, 1956, p. 441.
30. H. Guberman, Master's Thesis, Columbia University, 1958, Unpublished.
31. H. Schadler, AIME Trans., v. 218, 1960 p. 649.
32. N.J. Petch, Progress in Metal Physics, v. 5, 1954, p. 1.
33. G.W. Greenwood and A.G. Quarrell, J. Inst. Met., v. 82, 1953, p. 581.

34. F.E. Hauser, P.R. Landon and J.E. Dorn, AIME Trans., v. 206, 1956, p. 589.
35. N.J. Petch, Phil. Mag., v. 1, 1956, p. 186.
36. A. Seeger, Dislocations and Mechanical Properties of Crystals, Wiley, New York, 1957, p. 243.
37. M.W. Toaz and E.J. Ripling, AIME Trans., v. 206, 1956, p. 935.
38. F.E. Hauser, P.R. Landon and J.E. Dorn, ASM Trans., v. 48, 1956, p. 986.
39. J.J. Gilman, AIME Trans., v. 200, 1954, p. 621.
40. G.V. Raynor, Physical Metallurgy of Magnesium and its Alloys, Pergamon Press, New York, 1959.
41. A.T. Churchman, AIME Trans., v. 218, 1960, p. 262.
42. D. Harker, ASM Trans., v. 32, 1944, p. 210.
43. H. Aaronson and co-workers, Ford Scientific Laboratory, private communication.
44. A.N. Stroh, Phil. Mag., v. 3, 1958, p. 597.
45. A.N. Stroh, Phil. Mag., v. 46, 1955, p. 968.
46. A.H. Cottrell, AIME Trans., v. 212, 1958, p. 192.
47. A.R. Kaufmann, P. Gordon and D.W. Lillie, ASM Trans., v. 42, 1950, p. 785.
48. G.I. Taylor, J. Inst. Met., v. 62, 1938, p. 307.
49. J.J. Gilman, AIME Trans., v. 212, 1958, p. 783.
50. R.L. Bell and R.W. Cahn, J. Inst. Met., v. 86, 1958, p. 433.
51. J.J. Gilman, AIME Trans., v. 200, 1954, p. 621.
52. J.J. Gilman, Swampscott Fracture Conference, Wiley, New York, 1959.
53. A.A. Griffith, Phil. Trans. Roy. Soc., v. 221A, 1921, p. 163.

54. A.N. Stroh, Advances in Physics, v. 6, 1957, p. 418.
55. P.B. Price, Phil. Mag., v. 5, 1960, p. 873.
56. H.S. Rosenbaum, Gen. Electric Report No. 60-RL-(2536M), Oct. 1960.
57. H. Nichols and W. Restoker, Acta Met., v. 3, 1960, p. 788.

TABLE 1

## SLIP AND TWIN PLANES IN THE HEXAGONAL METALS

Metal	Axial Ratio	Slip Planes			Twin Planes		
		-196°C	20°C	Elevated Temp.	-196°C	20°C	Elevated Temp.
Cadmium	1.886	(0001)	$\begin{Bmatrix} 0001 \\ 11\bar{2}2 \end{Bmatrix}$	(0001)	(10 $\bar{1}$ 2)	(10 $\bar{1}$ 2)	(10 $\bar{1}$ 2)
Zinc	1.856	(0001)	$\begin{Bmatrix} 0001 \\ 11\bar{2}2 \end{Bmatrix}$	$\begin{Bmatrix} 0001 \\ 1010 \end{Bmatrix}$	(10 $\bar{1}$ 2)	(10 $\bar{1}$ 2)	(10 $\bar{1}$ 2)
Magnesium	1.623	$\begin{Bmatrix} 0001 \\ 10\bar{1}0 \\ 11\bar{2}2 \end{Bmatrix}$	$\begin{Bmatrix} 0001 \\ 10\bar{1}1 \\ 10\bar{1}0 \end{Bmatrix}$	(10 $\bar{1}$ 1)	(10 $\bar{1}$ 2)	$\begin{Bmatrix} 10\bar{1}2 \\ 30\bar{3}4 \end{Bmatrix}$	$\begin{Bmatrix} 10\bar{1}3 \\ 30\bar{3}4 \end{Bmatrix}$
Rhenium	1.61			$\begin{Bmatrix} 0001 \\ 10\bar{1}0 \\ 10\bar{1}1 \end{Bmatrix}$			$\begin{Bmatrix} 11\bar{2}1 \\ 11\bar{2}2 \\ 10\bar{1}2 \end{Bmatrix}$
Titanium	1.587	(10 $\bar{1}$ 0)	$\begin{Bmatrix} 10\bar{1}0 \\ 0001 \\ 10\bar{1}1 \end{Bmatrix}$	$\begin{Bmatrix} 10\bar{1}0 \\ 10\bar{1}1 \end{Bmatrix}$	$\begin{Bmatrix} 11\bar{2}4 \\ 11\bar{2}2 \\ 11\bar{2}3 \\ 11\bar{2}1 \end{Bmatrix}$	$\begin{Bmatrix} 11\bar{2}1 \\ 10\bar{1}2 \\ 11\bar{2}2 \end{Bmatrix}$	$\begin{Bmatrix} 11\bar{2}1 \\ 11\bar{2}2 \end{Bmatrix}$
Zirconium	1.585	(10 $\bar{1}$ 0)	(10 $\bar{1}$ 0)	(10 $\bar{1}$ 0)	$\begin{Bmatrix} 11\bar{2}1 \\ 11\bar{2}2 \\ 11\bar{2}3 \\ 10\bar{1}2 \end{Bmatrix}$	$\begin{Bmatrix} 11\bar{2}1 \\ 11\bar{2}2 \\ 11\bar{2}3 \\ 10\bar{1}2 \end{Bmatrix}$	$\begin{Bmatrix} 11\bar{2}1 \\ 11\bar{2}2 \\ 11\bar{2}3 \\ 10\bar{1}2 \end{Bmatrix}$
Beryllium	1.565		$\begin{Bmatrix} 10\bar{1}0 \\ 0001 \end{Bmatrix}$	$\begin{Bmatrix} 10\bar{1}0 \\ 0001 \end{Bmatrix}$		(10 $\bar{1}$ 2)	(10 $\bar{1}$ 2)

TABLE 2

## SPECTROGRAPHIC ANALYSES OF TEST MATERIALS

Impurity	Per Cent Analyzed		
	99.95 per cent Cadmium	99.99 + per cent Cadmium	99.97 per cent Magnesium
Pb	0.022	0.004	<0.001
Cu	0.003	0.0002	<0.002
Zn	<0.01	ND	<0.005
Fe	<0.001	0.0001	-----
Mn	-----	ND	<0.002
Mg	0.008	<0.0001	-----
Si	-----	ND	0.01
Sn	<0.001	ND	-----
Ag	-----	<0.0001	-----
Ca	-----	ND	<0.001
Bi	-----	0.0001	-----
Al	-----	ND	<0.01
Sb	-----	ND	-----

ND denotes "none detected"

----- denotes "not reported"

TABLE 3  
COMPOSITIONS AND AXIAL RATIOS OF CADMIUM-MAGNESIUM ALLOYS

Melt Number	Weight per cent Magnesium	Atomic per cent Magnesium	Axial Ratio at 310°C*	Axial Ratio at 25°C**
Pure Cadmium	0	0	1.900	1.886
I	1.96	8.51	1.86	1.86
II	4.95	19.42	1.77	----
III	2.90	12.13	1.83	1.83
IV	3.15	13.07	1.82	1.83
V	2.69	11.33	1.84	1.84
VII	15.35	45.59	1.64	----
VIII	3.70	15.12	1.80	----

\* Estimated from data of Hume-Rothery and Raynor<sup>25</sup>

\*\* Estimated from data of Edwards, Wallace and Craig<sup>24</sup>

TABLE 4

## TENSILE PROPERTIES OF POLYCRYSTALLINE 99.95 PER CENT CADMIUM

No.	Grain Size in.	Temp. °C	Yield Stress psi	Tensile Strength psi	Fracture Strength psi	Plastic Strain per cent	Reduction in Area per cent
Cd-62	.0086	22	4520	7630	---	34.7	100
Cd-8	.015	22	2540	6300	---	31.8	100
Cd-61	.010	22	3640	8370	---	38.3	100
Cd-68	.0450	22	1350	4500	---	----	---
Cd-64	.011	22	3800	8550	---	----	---
Cd-60	.025	-38	3100	9190	---	----	100
Cd-7	.020	-77	3600	14,700	---	37.8	97.6
Cd-15	.008	-98	6200	17,600	---	42.9	91.8
Cd-58	.016	-114	3600	15,400	---	36.9	---
Cd-16	.008	-124	6950	21,700	---	44.4	91.5
Cd-21	.020	-140	3800	17,800	39,000	38.2	86.8
Cd-18	.007	-142	7600	21,000	49,200	36.2	78.8
Cd-12	.008	-148	4020	23,700	---	34.5	73.0
Cd-25	.020	-156	4000	20,650	38,200	28.6	52.9
Cd-19	.007	-154	8200	23,500	38,100	27.4	47.8
Cd-56	.0136	-157	5070	27,500	---	24.9	---
Cd-17	.008	-162	7300	27,900	34,400	26.1	39.5
Cd-23	.020	-171	4200	22,900	26,700	20.3	25.5
Cd-10	.007	-171	7200	29,700	37,000	26.8	33.1
Cd-13	.008	-177	7100	29,150	36,300	23.3	22.0
Cd-11	.008	-182	5800	29,500	35,200	17.6	16.1
Cd-59	.016	-187	3600	22,900	---	17.3	---
Cd-24	.020	-189	3200	20,700	24,600	15.7	19.4
Cd-14	.010	-196	5000	25,500	30,900	16.8	17.7
Cd-28	.0098	-196	6000	30,000	36,100	15.3	14.4
Cd-29	.0161	-196	3900	20,400	22,200	12.7	19.7
Cd-27	.029	-196	2300	17,700	19,100	16.1	21.1
Cd-9	.0076	-196	5980	31,700	28,200	14.3	---
Cd-63	.0073	-196	7410	---	---	----	---
Cd-45	.030	-269	2600	20,400	24,900	14.9	19.3
Cd-40*	.013	-269	4700	29,700	34,500	12.8	14.2

\* Strain rate = 0.1 in./in./min.

TABLE 5

## TENSILE PROPERTIES OF POLYCRYSTALLINE 99.99 + PER CENT CADMIUM

No.	Grain Size in.	Temp. °C	Yield Stress psi	Tensile Strength psi	Fracture Strength psi	Plastic Strain per cent	Reduction in Area per cent
A-3	.020	-146	3400	---	---	---	---
A-2	.020	-151	3320	24,800	33,500	27.9	47.2
A-4	.015	-171	3640	24,900	31,100	23.2	33.9
A-6	.023	-196	3910	22,500	26,200	15.8	14.8
A-1	.018	-196	5230	31,700	---	17.2	---
A-7*	.021	-196	---	---	---	---	14.6
A-12	.030	-196	1390	---	---	---	---

\* Strain rate: 20 in./in./min.



TABLE 6

## TENSILE PROPERTIES OF POLYCRYSTALLINE CADMIUM-MAGNESIUM ALLOYS

No.	Grain Size in.	Temp. °C	Yield Stress psi	Tensile Strength psi	Fracture Strength psi	Plastic Strain per cent	Reduction in area per cent
MELT I - 1.96 per cent Mg.							
I-4	.025	-77	7430	24,700	141,000	28.7	90.5
I-1	.030	-196	7980	21,700	25,700	9.9	15.5
MELT V - 2.69 per cent Mg							
V-8*	.0148	22	9760	14,790	---	30.9	80.5
-9	.0134	-45	12,600	21,900	31,600	24.1	74.0
-5		-73	11,400	27,600	48,700	28.7	72.3
-11	.0133	-84	9480	26,190	57,800	26.3	73.5
-10	.0184	-98	15,500	29,450	32,600	10.4	20.4
-3	.016	-113	15,300	31,200	35,600	10.9	17.8
-6	.016	-113	12,200	26,050	30,600	7.9	15.2
-1	.014	-146	9880	24,450	28,100	10.3	18.3
-2	.014	-171	11,400	23,900	27,900	8.2	13.6
-4*	.014	-196	16,600	26,600	30,200	4.6	11.7
MELT III - 2.90 per cent Mg							
III-1*	.016	22	7200	14,000	6600	---	92.3
-2	.013	-77	12,250	29,700	68,100	27.1	72.2
-8	.013	-113	8600	27,300	33,400	20.7	49.4
-6	.013	-151	11,150	29,400	35,700	12.6	21.4
-7	.018	-171	18,400	---	33,900	8.7	---
-4	.011	-196	18,000	29,100	33,100	6.5	12.2
MELT IV - 3.15 per cent Mg							
IV-17*	.0139	22	12,000	15,500	---	37.3	100
-2	.009	-77	14,100	28,400	79,500	32.6	78.8
-15	.0149	-98	---	31,900	37,400	12.9	16.5
-7	.0107	-113	16,000	30,050	24,700	16.4	21.0
-11	.0115	-134	19,200	31,900	38,400	8.9	17.0
-6	.0103	-151	17,000	29,000	35,700	10.3	22.3
-12	.020	-171	14,400	23,500	25,100	6.62	7.0
-14	.019	-196	11,600	20,400	22,100	6.63	10.2
-4	.010	-196	16,600	24,600	27,500	4.75	10.4
-18	.025	-269	14,300	22,000	21,100	3.73	18.8

TABLE 6 (Cont'd)

## TENSILE PROPERTIES OF POLYCRYSTALLINE CADMIUM-MAGNESIUM ALLOYS

No.	Grain Size in.	Temp. °C	Yield Stress psi	Tensile Strength psi	Fracture Strength psi	Plastic Strain per cent	Reduction in area per cent
MELT II - 4.95 per cent Mg.							
II-9**	.052	22	6,820	21,000	24,800	3.85	15.1
-6**	.038	22	16,500	23,500	27,900	3.41	28.4
-3	.015	22	----	24,500	40,700	----	39.9
-4**	.015	77	11,800	32,100	38,200	----	14.9
-7**	.036	-122	24,700	31,950	38,500	1.23	15.9
-5	.030	-196	24,700	34,300	37,400	1.26	8.74
-1	.020	-196	----	38,000	43,400	----	15.4
MELT VII - 15.35 per cent Mg.							
VII-8	.021	-126	18,800	33,400	62,800	15.6	16.6
-2	.021	-149	27,450	45,800	58,300	8.1	22.9
-6	.020	-166	26,600	49,600	58,200	10.8	14.6
-4	<.007	-196	28,700	50,700	57,500	7.0	11.7

- ° Strain rate: 0.1 in./in./min.
- \*\* Water quenched
- \* Yield point observed
- \*\* Test interrupted

TABLE 7

## TRANSITION TEMPERATURE VS. ALLOY CONTENT

Material	Weight per cent Magnesium	Temp. for 50 per cent Reduction in Area °C	Temp. for 20 per cent Reduction in Area °C
Cadmium	0	-155	-182
Melt I	1.96	----	----
Melt V	2.69	-83	-105
Melt III	2.90	-115	-155
Melt IV	3.15	-93	-105
Melt II	4.95	> 22	~ 22*
Melt VII	15.35	----	----

\* grain size dependent

TABLE 8

## TWINNING OF 99.99 + PER CENT CADMIUM SINGLE CRYSTALS

Number	$\alpha$ .	$\lambda$ .	Temp. °C	Normal Stress First Twin psi	Normal Stress Relaxed Twin psi
Cd-10-1	4	18	22	1080	610
-2	4	18	22	980	610
-3	4	18	22	760	580
-4	4	18	22	700	270
-5	4	18	22	660	570
Cd-11-2	4	13	22	850	720
-3	4	13	100	780	680
-5	4	13	100	720	705
Cd-12-1	3	13	110	740	510
-3	3	13	22	740	660
-4	3	13	80	650	450
Cd-13-3	5	28	140	580	530
Cd-14-1	3	21	80	2820	190
-2	3	21	110	940	570
-3	3	21	150	3270	---
-4	3	21	22	990	890
Cd-15-2	4	27	160	610	540
-4	4	27	160	1060	630

TABLE 9

## TWINNING OF 99.95 PER CENT CADMIUM SINGLE CRYSTALS

Number	$\chi_0$	$\lambda_0$	Temp. °C	Normal Stress First Twin psi	Normal Stress Relaxed Twin psi
Cd 1-1	3	2	22	2990	1140
-2	3	2	22	1430	1270
-4	3	2	22	850	670
-5	3	2	22	2050	710
Cd 8-1	5	5	100	980	640
-2	5	5	100	660	590
-3	5	5	100	840	465

TABLE 10

## IDENTIFICATION OF SLIP TRACES

Specimen No.	Orientation of Crystal*		Method of Test	Temp. °C	Planes
	$\chi_0$	$\lambda_0$			
Cd 44-1 a)	3	2	Scratch	-196	(11 $\bar{2}2$ )( $\bar{1}\bar{1}22$ )
Cd-44-1 b)	5	9	Scratch	-196	(11 $\bar{2}2$ )( $\bar{1}\bar{1}22$ )
Cd-44-2	3	2	Scratch	-196	(11 $\bar{2}2$ )( $\bar{1}\bar{1}22$ )
Cd-42-2	3	5	Bend	-196	( $\bar{1}\bar{1}22$ )
Cd-30-3	3	15	Bend	22	( $\bar{1}\bar{1}22$ )
Cd-46-1	1	5.5	Compression	22	(11 $\bar{2}2$ )
Cd-46-2	1	6.5	Compression	22	(11 $\bar{2}2$ )
Cd-46-3	1	6	Compression	-196	( $\bar{1}\bar{1}22$ )
Cd-31-5	2	9	Compression	-196	**
Cd-30-4	3	15	Compression	-196	**
Cd-40-4	4	5	Compression	22	(11 $\bar{2}2$ )( $\bar{1}\bar{1}22$ )

\* If bicrystal or tricrystal, orientation refers only to grain analyzed.

\*\* Traces too faint for analysis, but resembled traces on other crystals.

TABLE 11

## DUCTILITY TRANSITIONS IN HEXAGONAL METALS

Metal	Melting Point °C	Axial Ratio	Transition Temp. °C per cent MP		Probable Cause of Transition
Cadmium	321	1.886	-155	19.7	recovery, increased hardening
Zinc	419	1.856	50	46.7	recovery
Magnesium	650	1.624	150	65.2	recrystallization
Titanium	1820	1.587	none	----	----
Zirconium	1750	1.585	none	----	----
Beryllium	1280	1.565	600	56.2	impurities

TABLE 12

## COMPARISON OF EFFECTIVE SURFACE ENERGIES FOR HEXAGONAL METALS

Metal	$\Sigma$ dynes/cm <sup>2</sup> $\times 10^{12}$	$k$ (dynes/cm <sup>2</sup> )cm <sup>1/2</sup> $\times 10^8$	$\gamma = \frac{E}{2\sigma_0} \left(\frac{a'}{\pi}\right)^2$ ergs/cm <sup>2</sup>	$\gamma_c = \frac{k^2}{E}$ ergs/cm <sup>2</sup> $\times 10^4$	$\frac{\gamma_c}{\gamma}$
Cadmium	0.28	3.34	224	39.9	1780
Zinc a)	0.35	0.94	254	2.53	99.5
Zinc b)	0.35	0.92	254	2.42	95.3
Zinc c)	0.35	0.17	254	0.083	3.25
Magnesium <sup>d)</sup>	0.43	0.85	430	1.68	39.2

\* Taken from Griffith condition:  $\sigma_F \approx \sqrt{\frac{E\gamma_c}{c}}$

a) Present investigation

b) Greenwood and Quarrell<sup>33</sup>

c) Petch<sup>32</sup>

d) Hauser, Landon and Dorn<sup>34</sup>



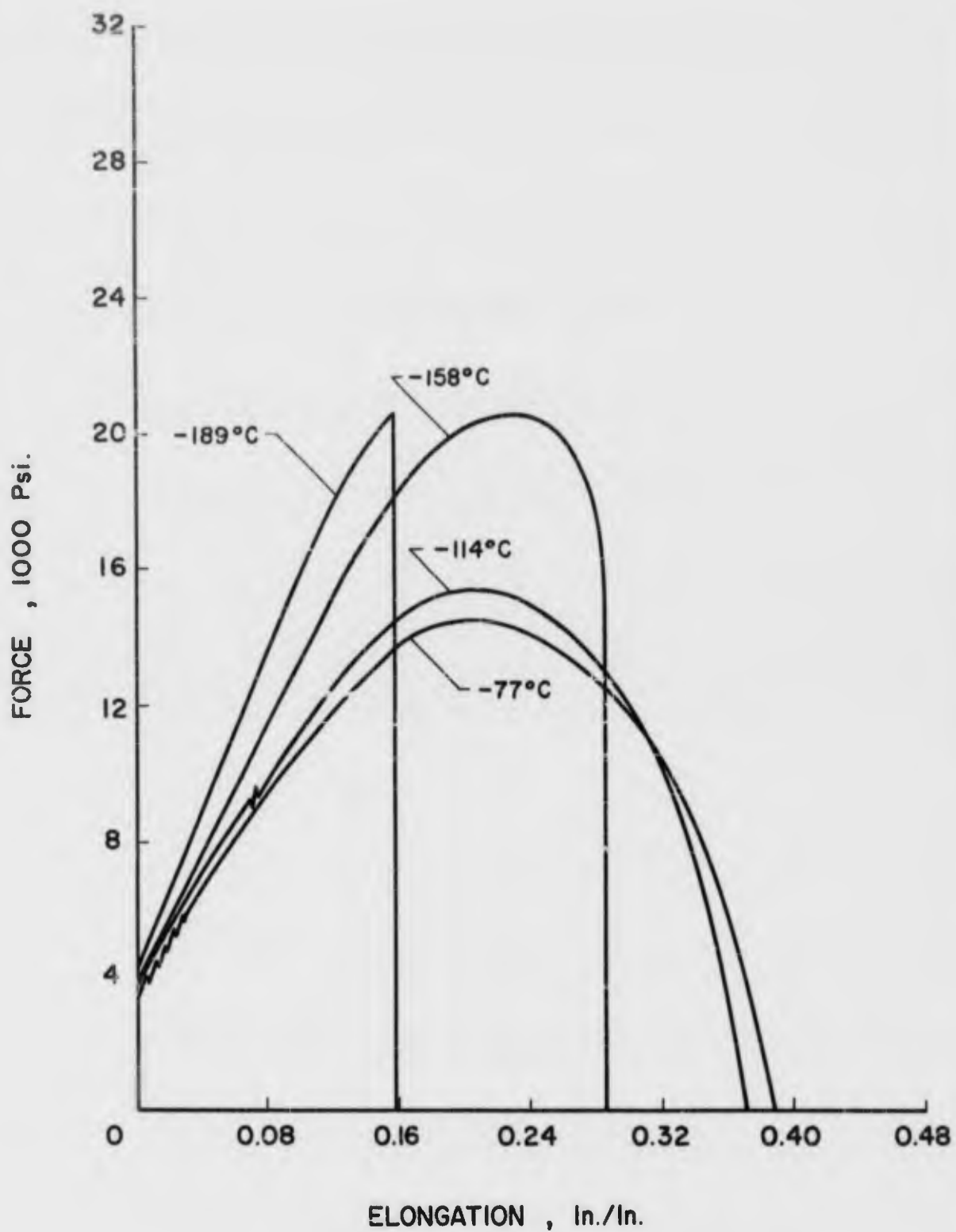


FIG. 1. FORCE - ELONGATION CURVES FOR CADMIUM  
AT SEVERAL TEMPERATURES ( $d = 0.020$ " )

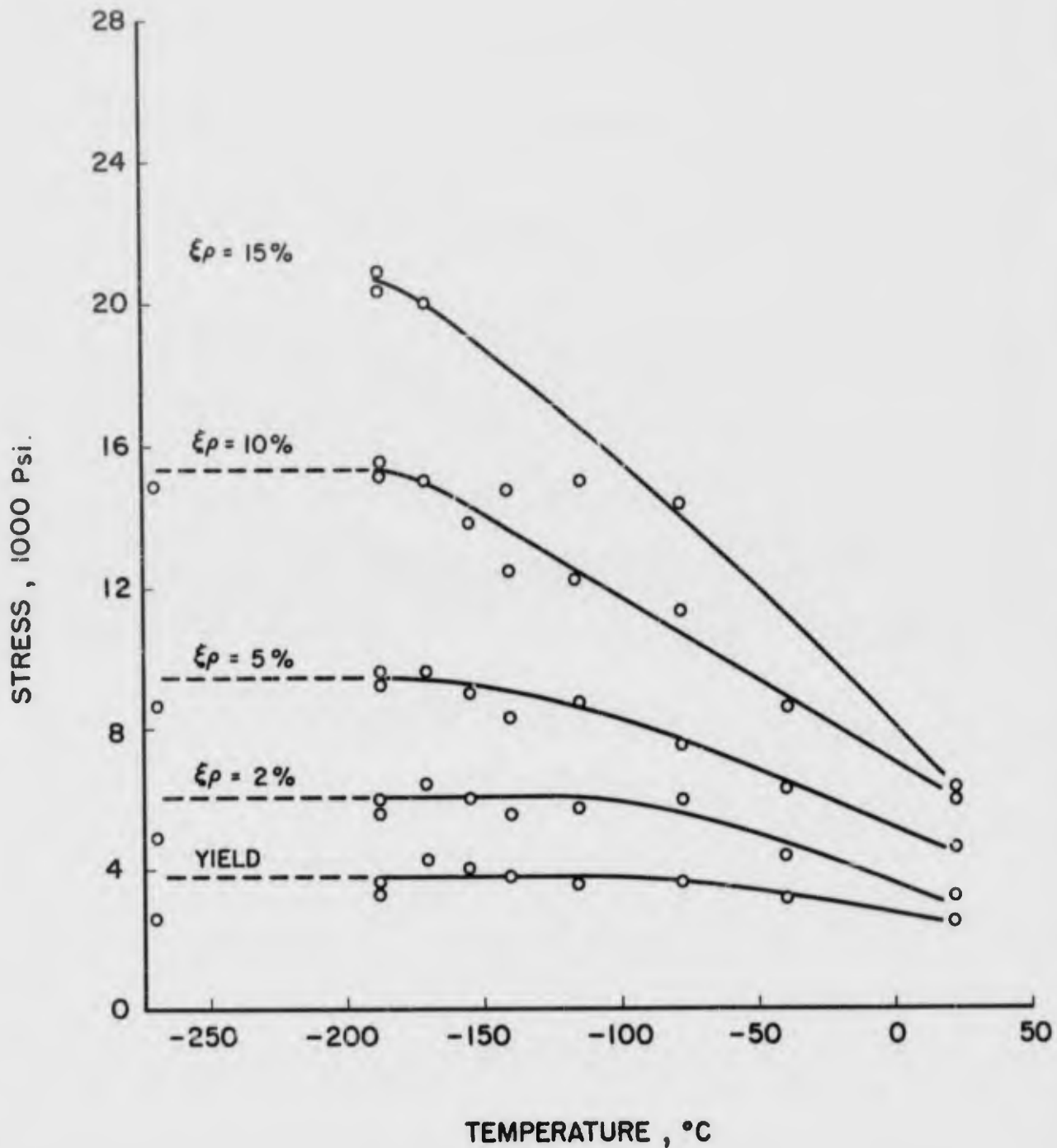


FIG. 2. EFFECT OF TEMPERATURE ON FLOW STRESS FOR CADMIUM ( $d = 0.020''$ )

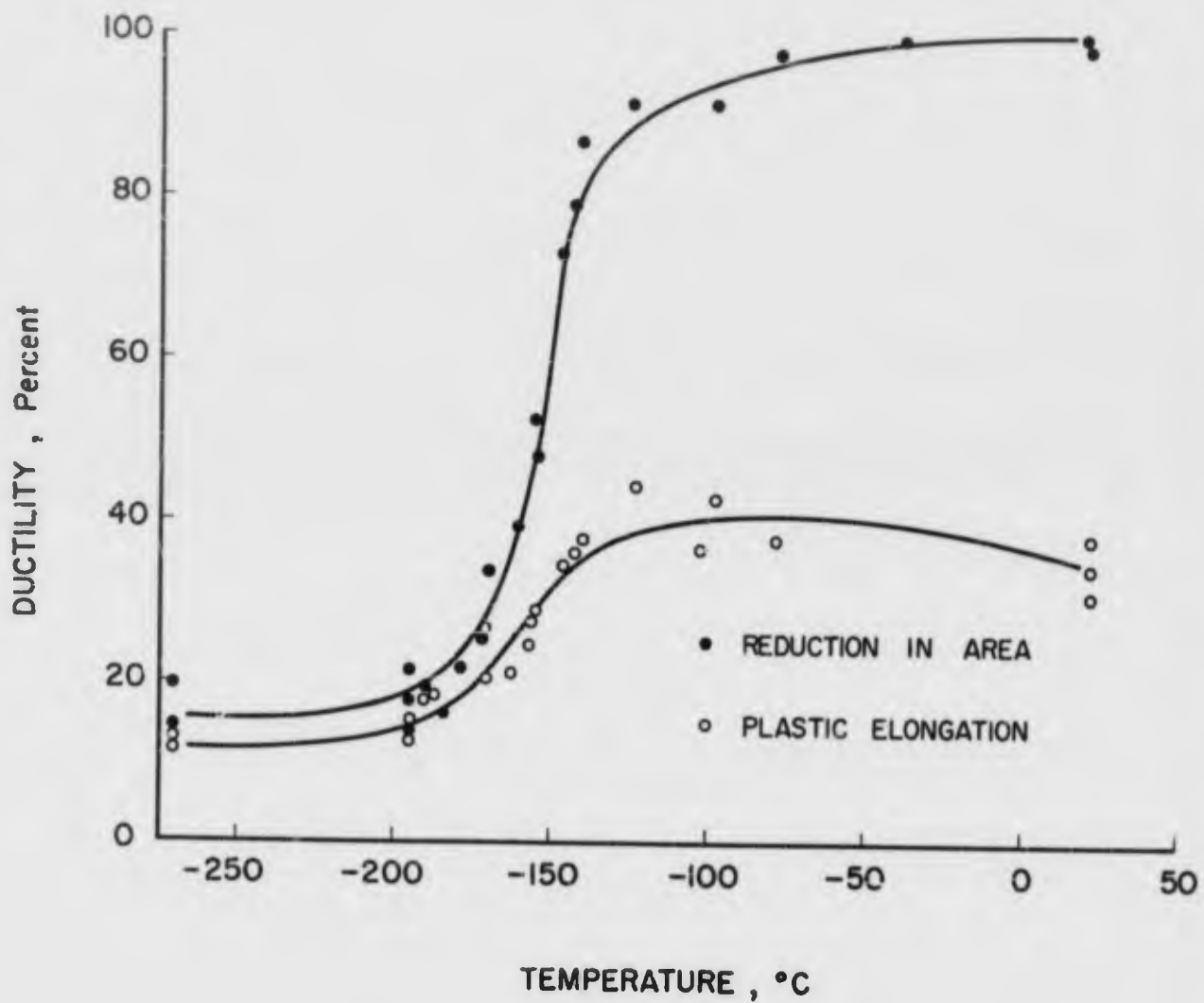


FIG. 3 . EFFECT OF TEMPERATURE ON DUCTILITY OF CADMIUM

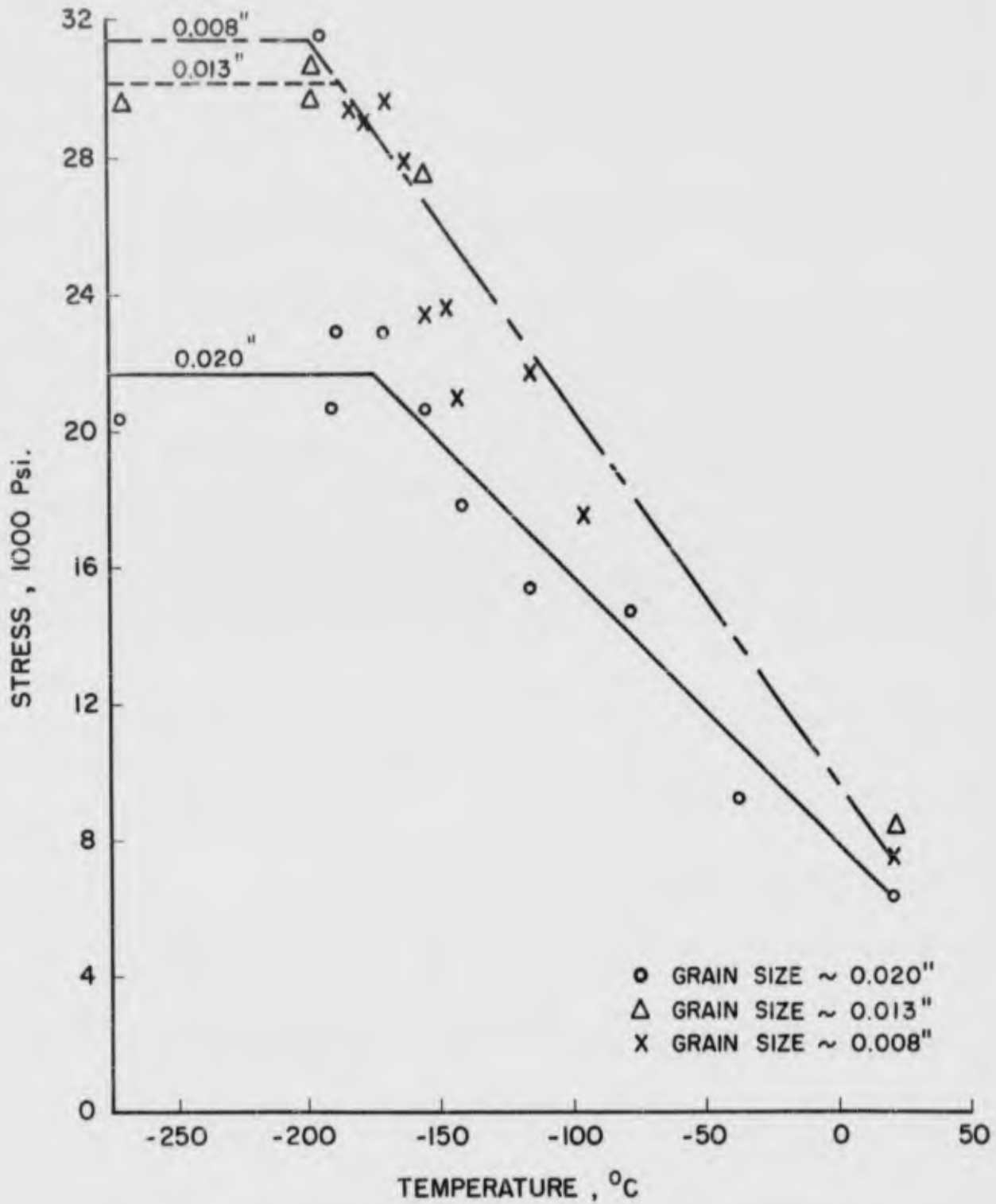


FIG. 4. TENSILE STRENGTH VS. TEMPERATURE FOR CADMIUM

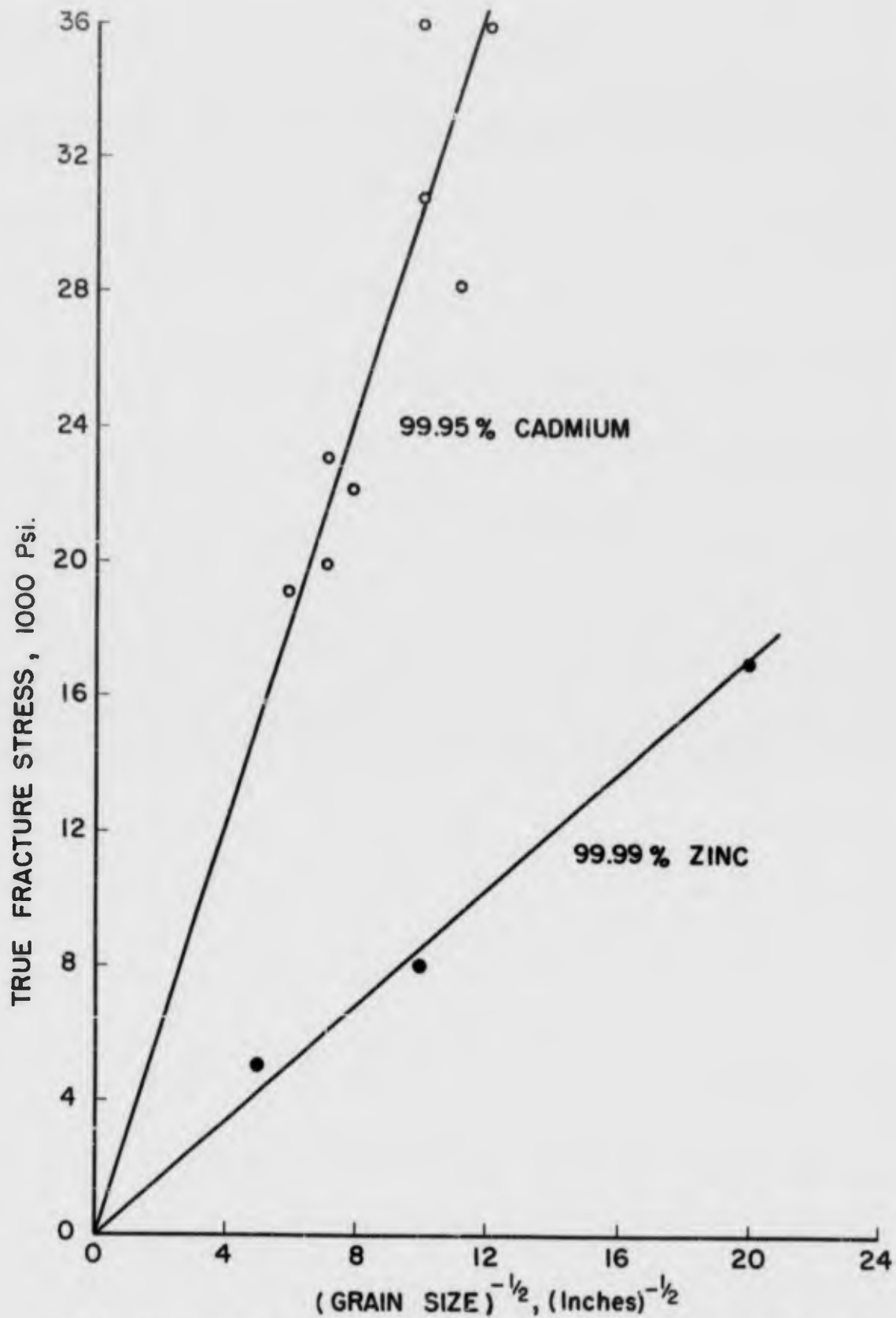


FIG 5. EFFECT OF GRAIN SIZE ON FRACTURE STRESS (FOR CADMIUM AND ZINC)

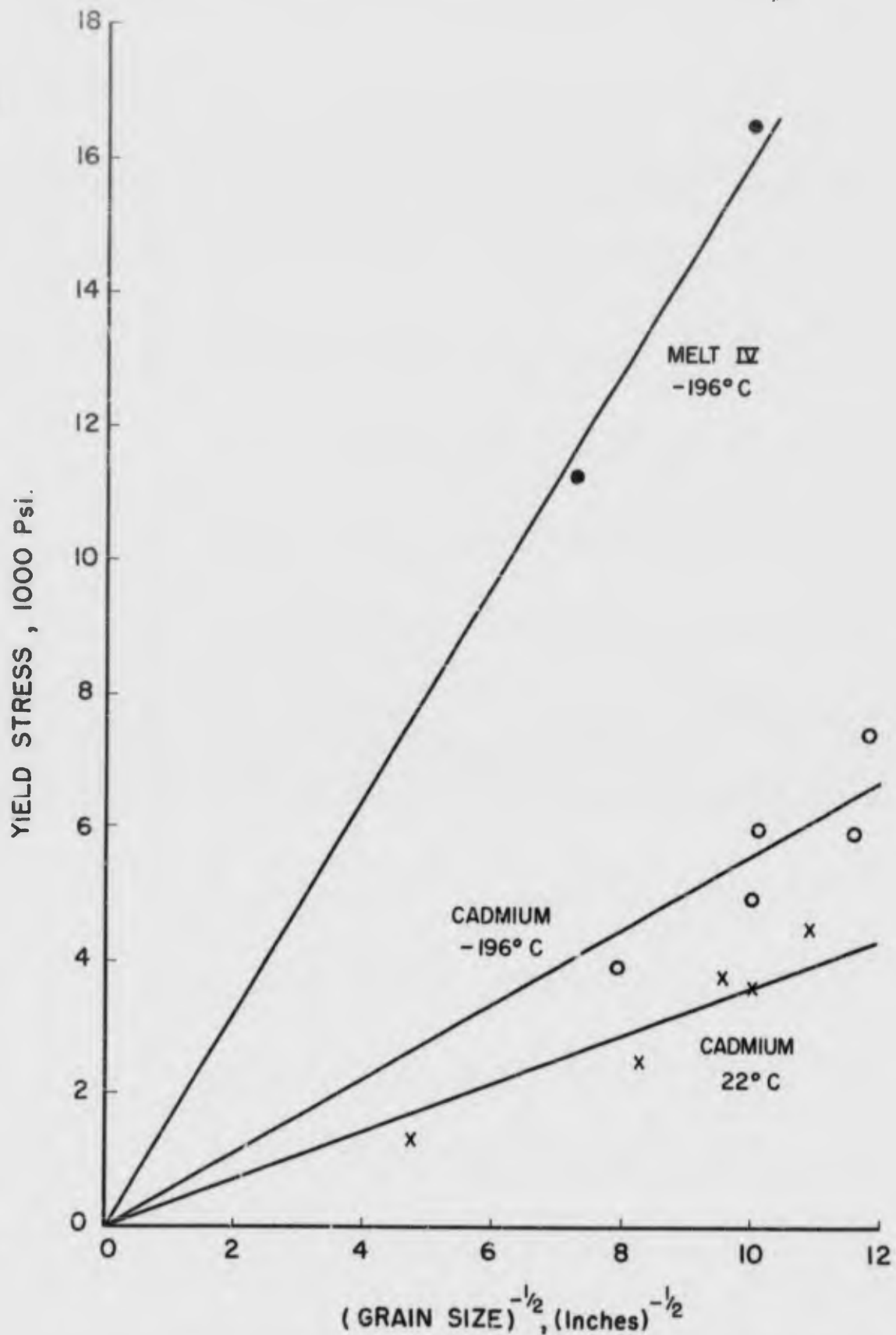


FIG. 6. EFFECT OF TEMPERATURE AND GRAIN SIZE ON YIELD STRESS (OF CADMIUM)

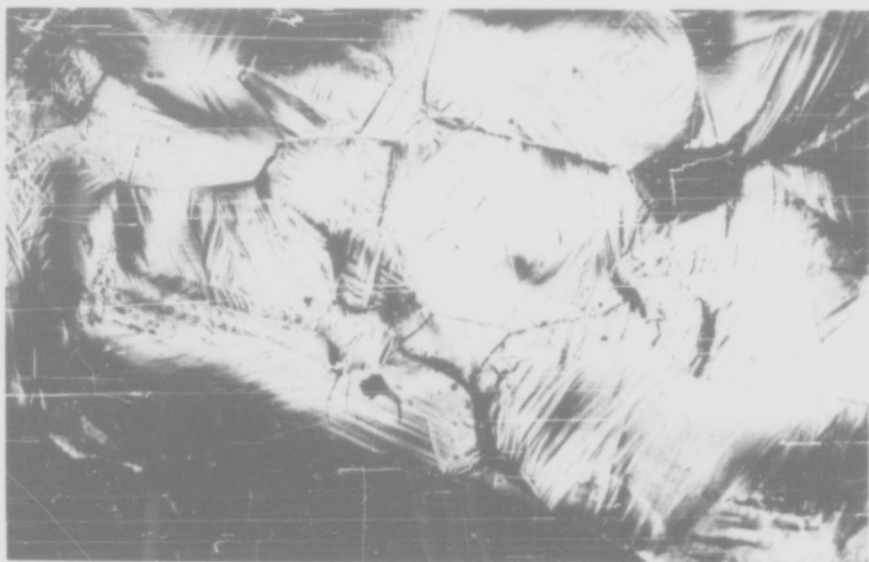


Fig. 7 Microstructure of polycrystalline cadmium, specimen Cd-40, tested in tension to fracture at 4.2°K, x150

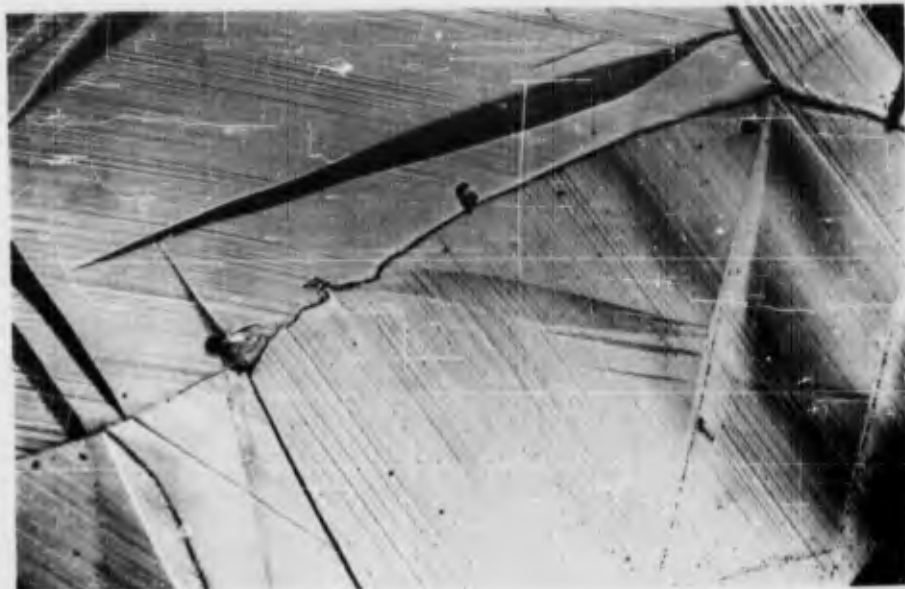
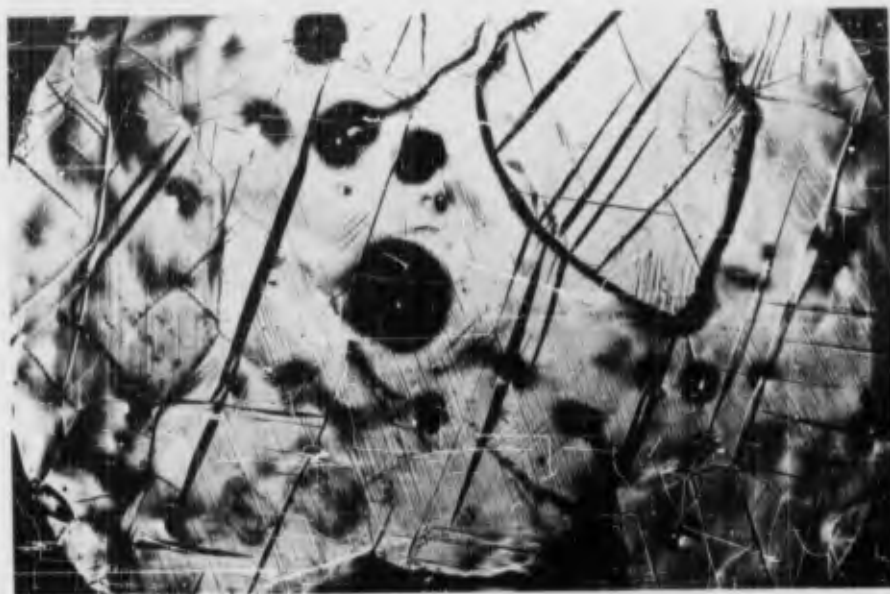


Fig. 8 Basal slip and twinning in polycrystalline cadmium, specimen Cd-S-11, strained 16 per cent in compression at room temperature, x150





a)



b)

Fig. 9 Slip and twin traces in polycrystalline cadmium, tested in compression at  $-196^{\circ}\text{C}$  a) specimen Cd-S-12, 20 per cent strain, x50 b) specimen Cd-S-2, 15 per cent strain, x150

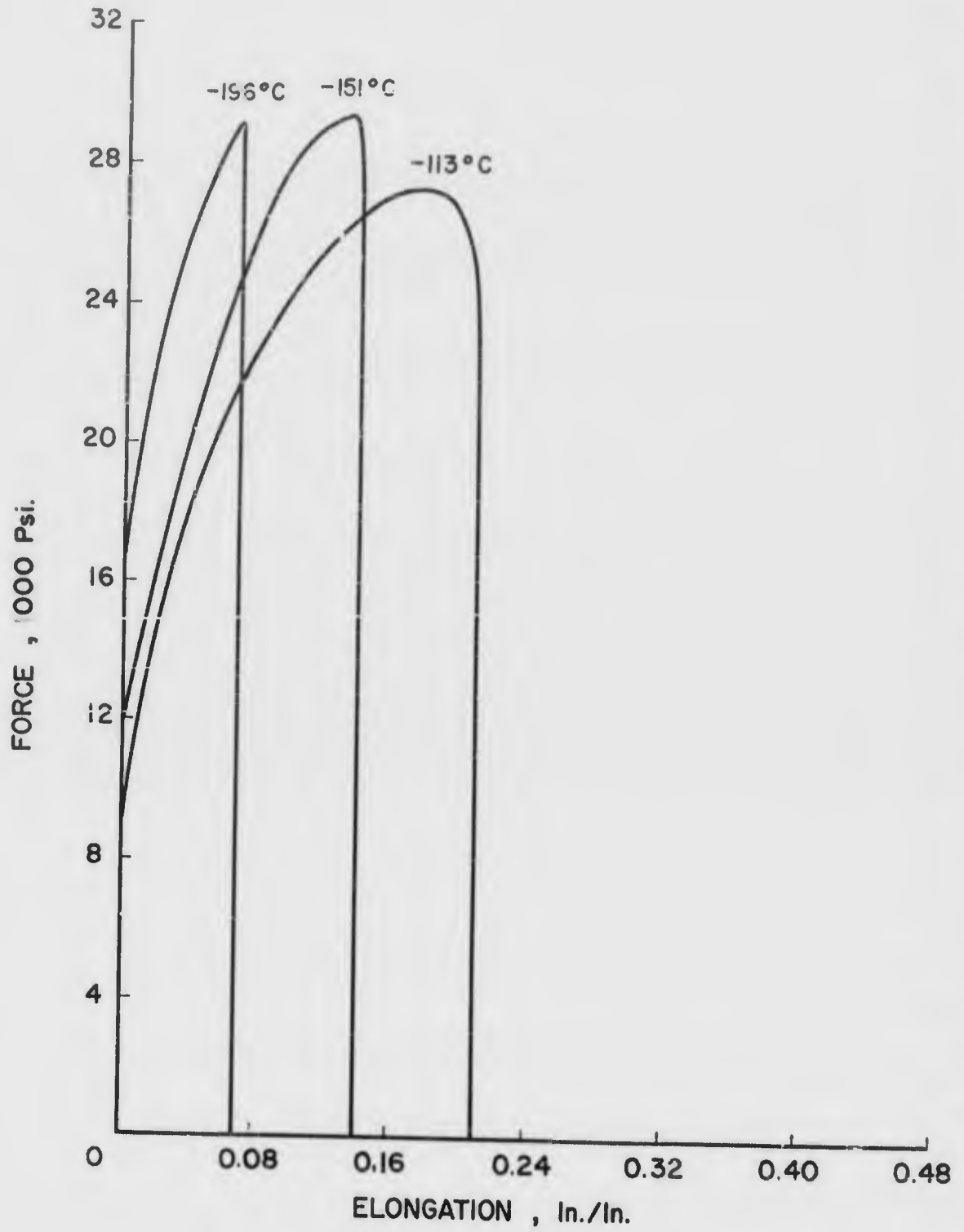


FIG.10. FORCE - ELONGATION CURVES FOR CADMIUM  
2.90% MAGNESIUM ALLOY , MELT III

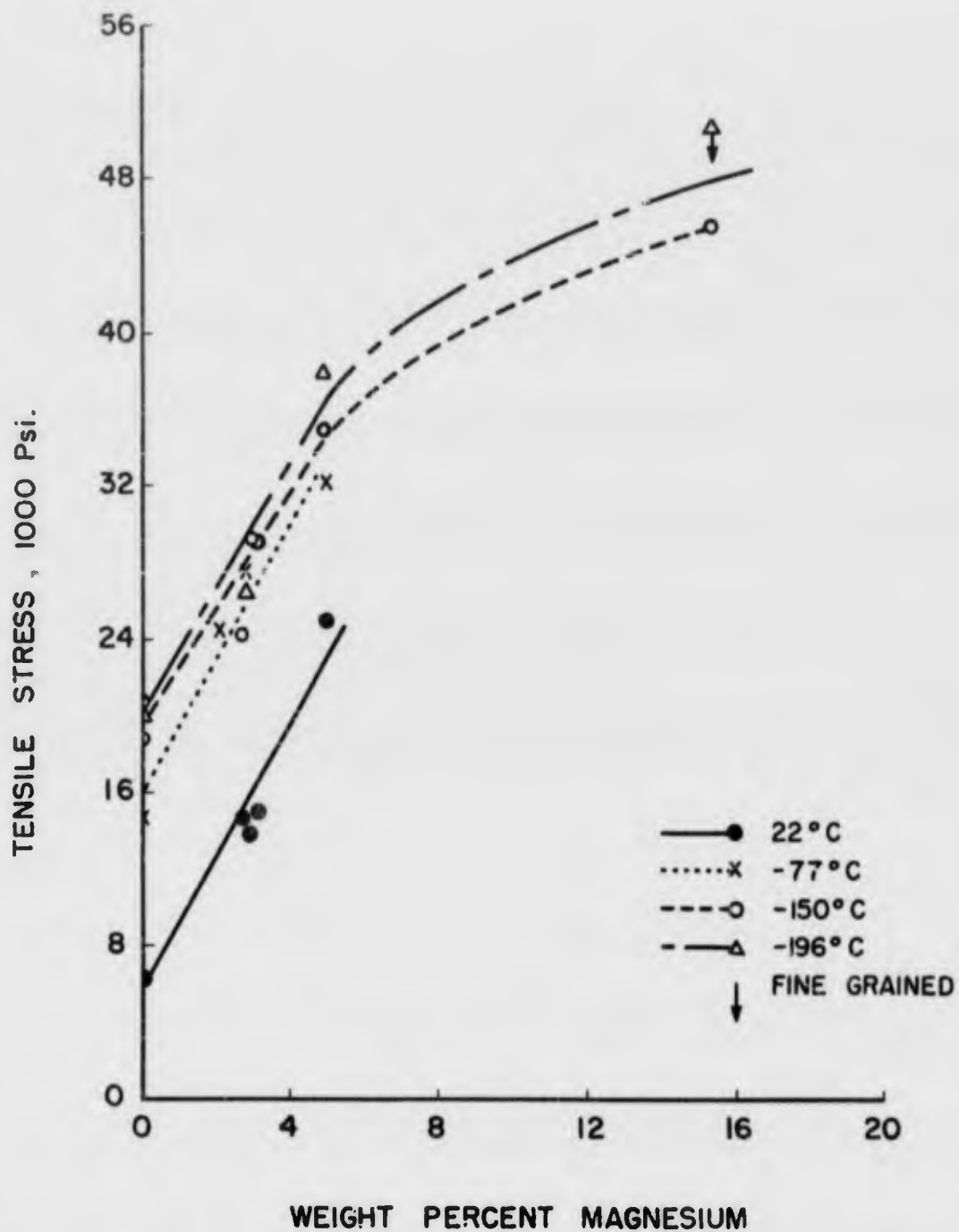


FIG. 11. EFFECT OF ALLOY CONTENT ON TENSILE STRENGTH OF CADMIUM ( $d=0.015''$ )

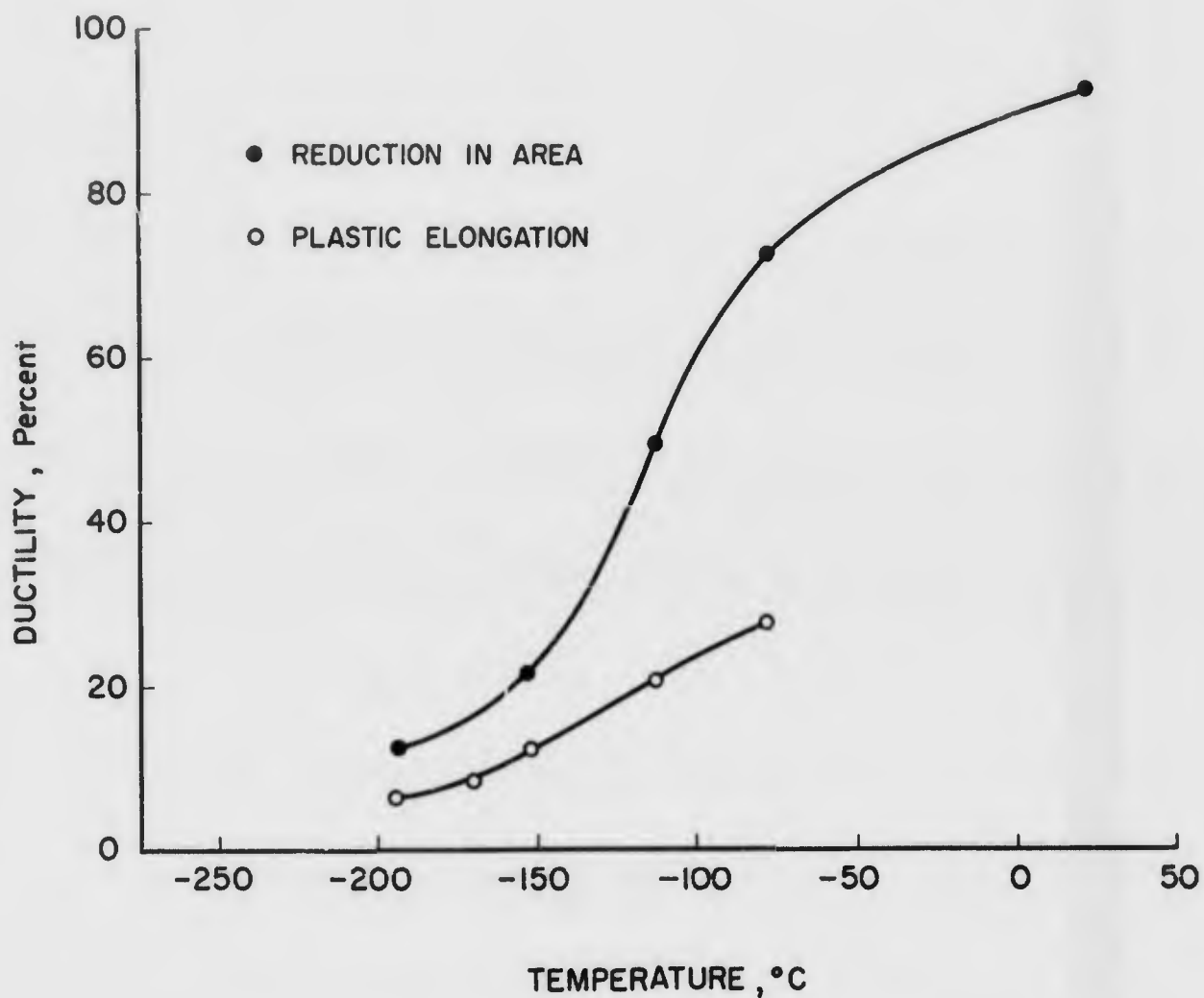


FIG.12. EFFECT OF TEMPERATURE ON DUCTILITY OF CADMIUM  
2.90% MAGNESIUM ALLOY, MELT III

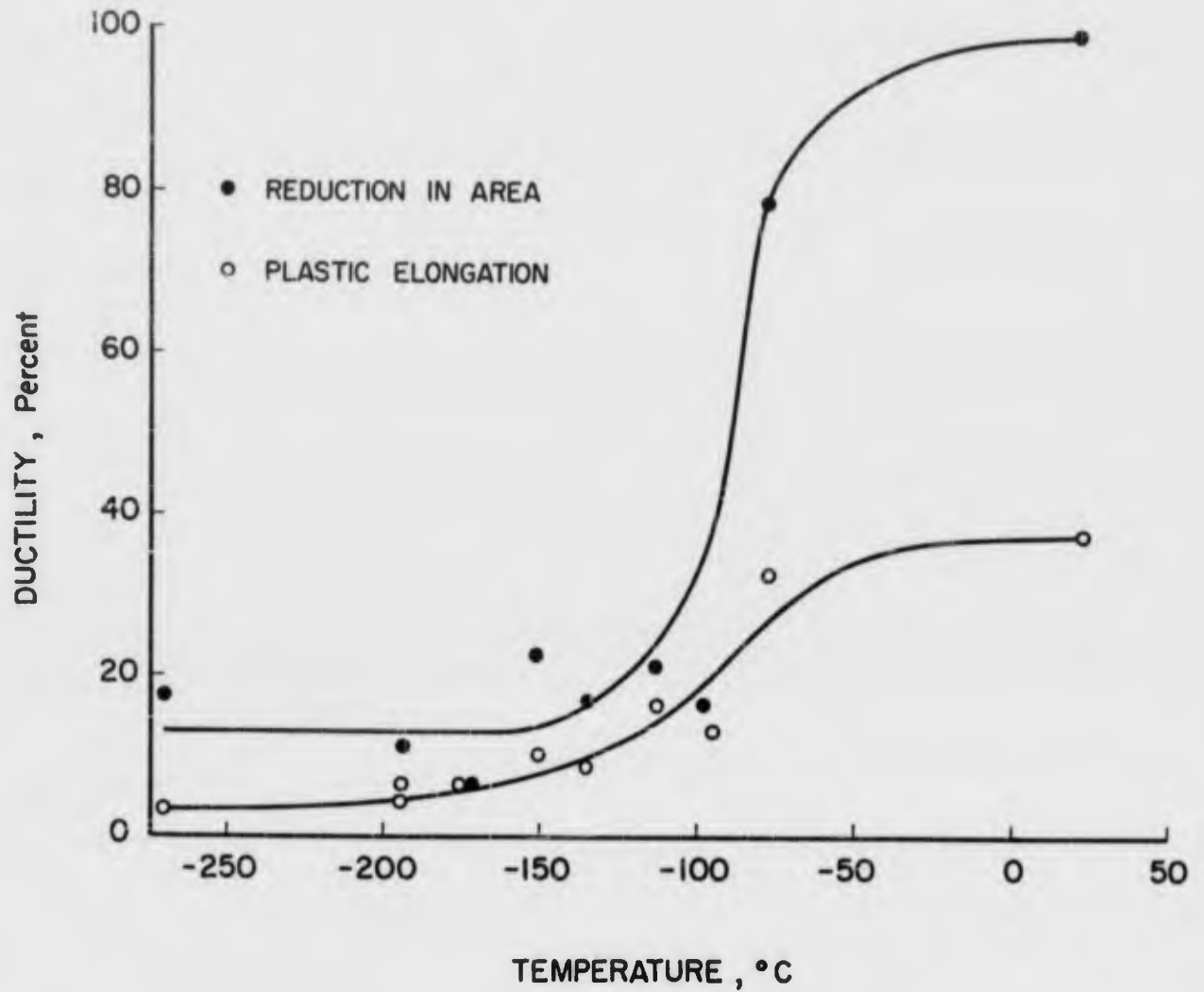


FIG. 13. EFFECT OF TEMPERATURE ON DUCTILITY OF CADMIUM  
3.15 % MAGNESIUM ALLOY, MELT IV

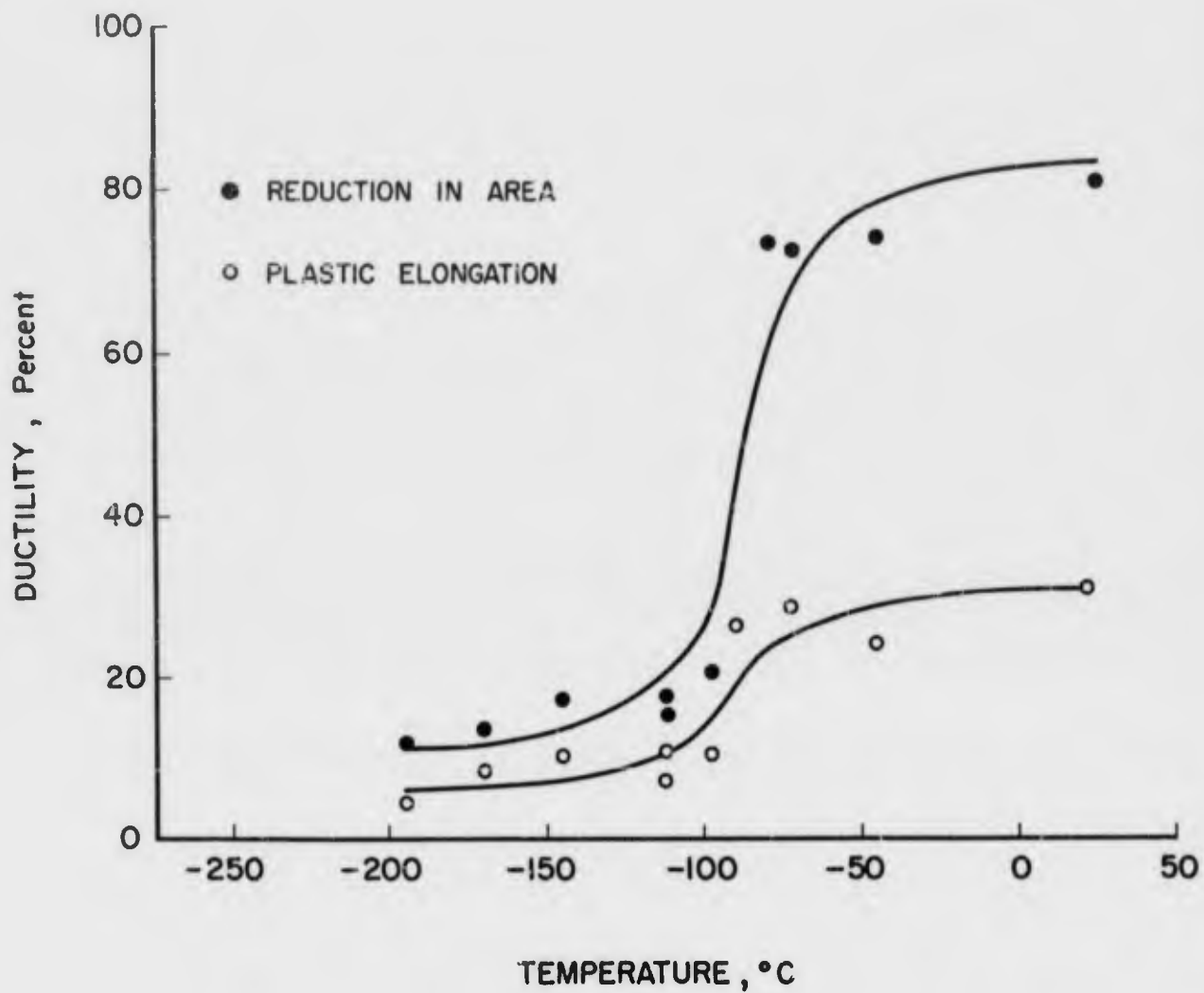
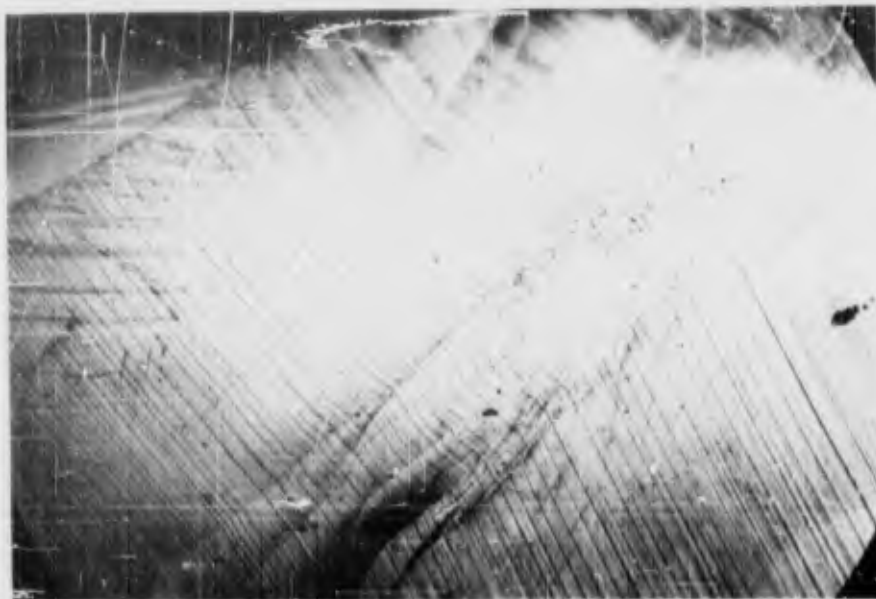
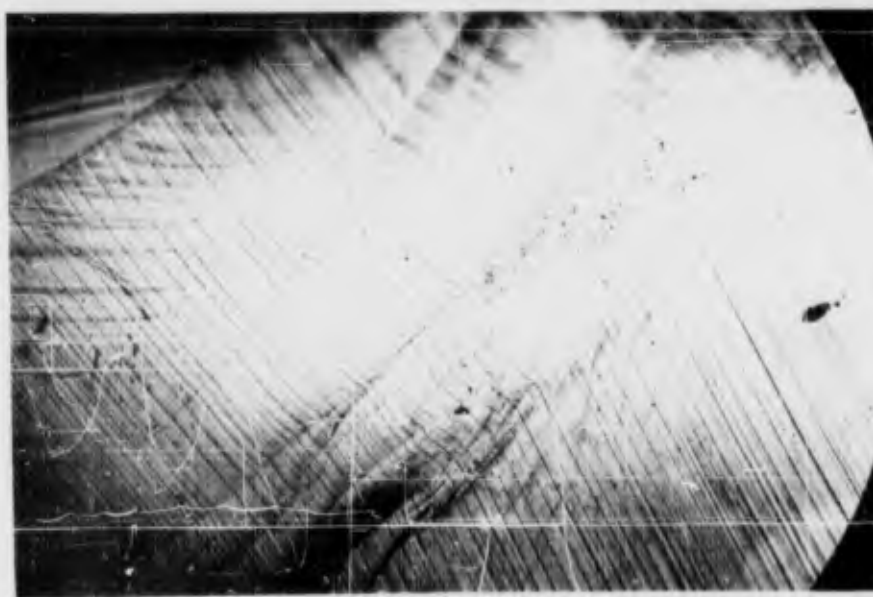


FIG. 14. EFFECT OF TEMPERATURE ON DUCTILITY OF CADMIUM  
2.69% MAGNESIUM ALLOY, MELT V



a)

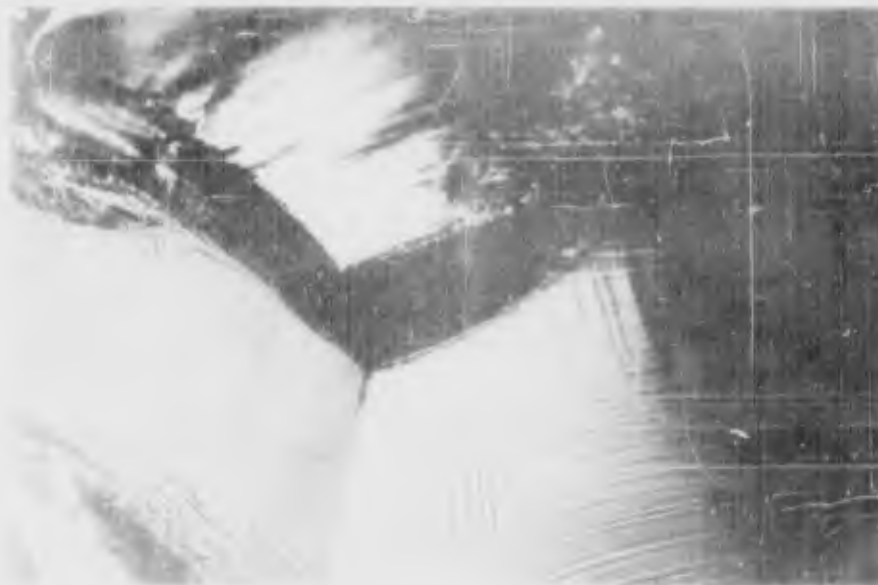


b)

Fig.15 Kinking, slip and twinning in cadmium -3.15 per cent magnesium alloy, specimen IV-18, tested in tension to fracture at  $4.2^{\circ}\text{K}$  a) x200 b) x200



a)



b)

Fig.16 Deformation markings and intergranular fracture in cadmium  
-3.15 per cent magnesium specimen IV-14, tested in tension  
at  $-196^{\circ}\text{C}$ . a) x200 b) x200



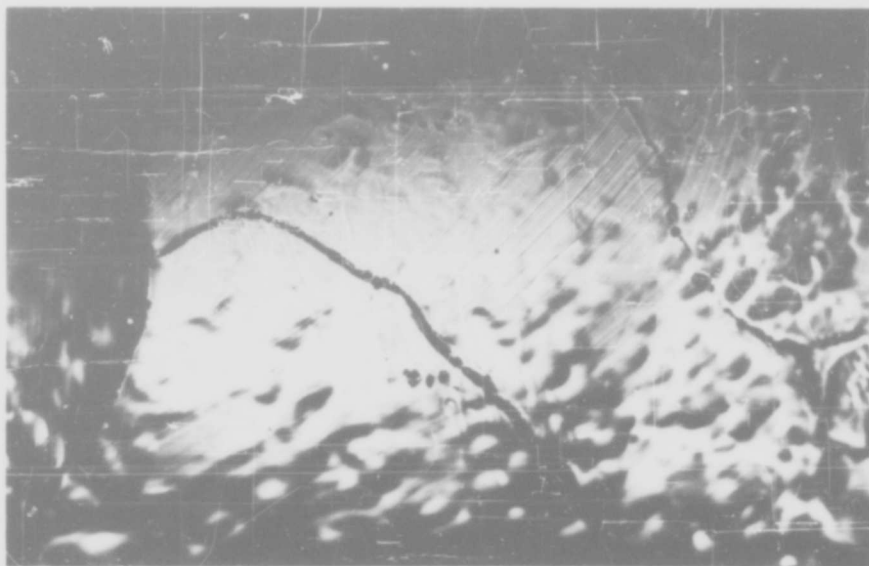
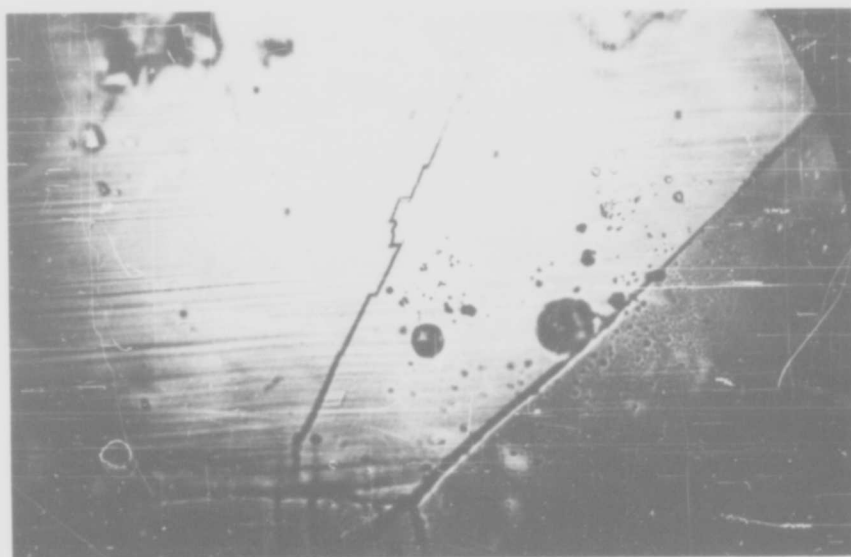


Fig.17 Slip and twinning in cadmium -4.95 per cent magnesium alloy, specimen II -9, strained 2 per cent in tension at room temperature, x150



a)



b)

Fig. 18 Slip traces in cadmium - 4.95 per cent magnesium alloy, specimen II-7, tested in tension to fracture at  $-122^{\circ}\text{C}$ . Basal slip traces predominant a) x 200 b) x500

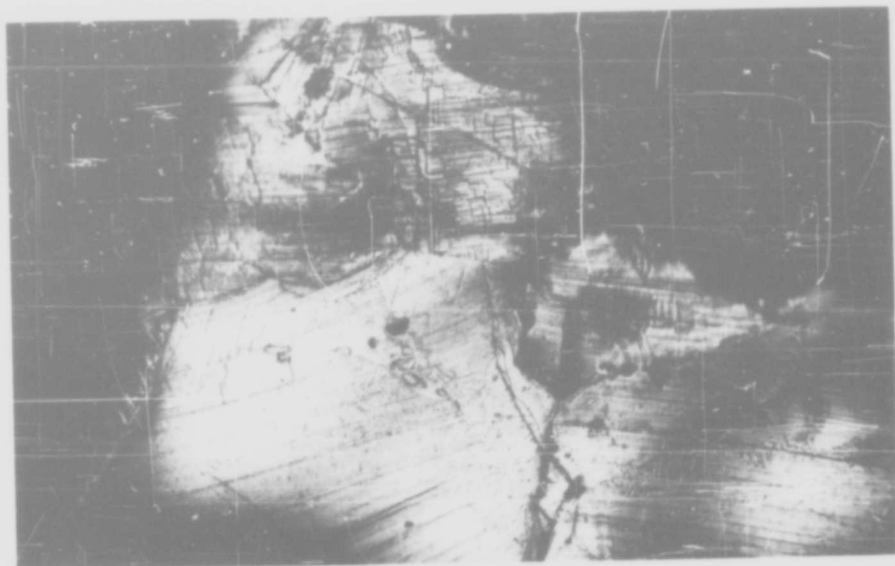


Fig. 19 Slip traces in cadmium - 4.95 per cent magnesium alloy, specimen II-4, tested in tension at  $-196^{\circ}\text{C}$ . View is adjacent to fracture surface at upper right, x 150

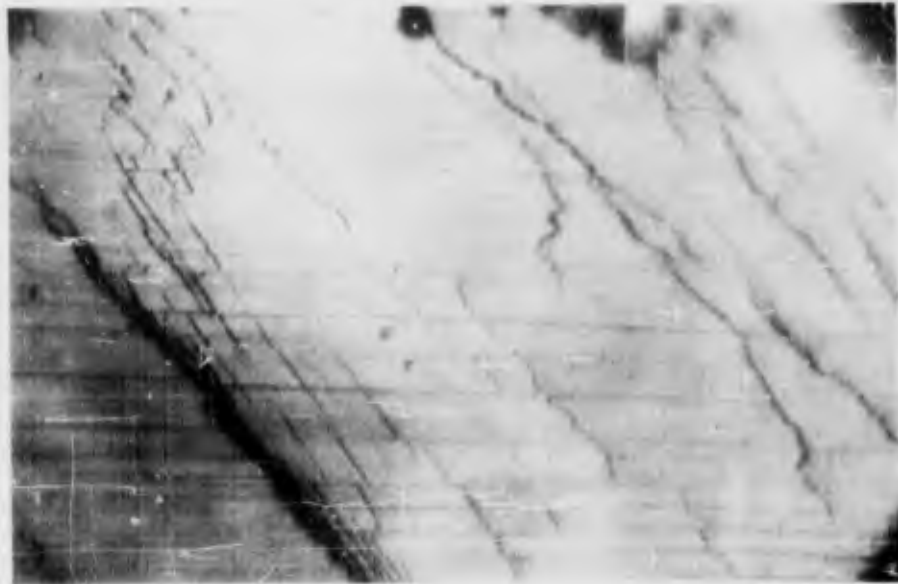
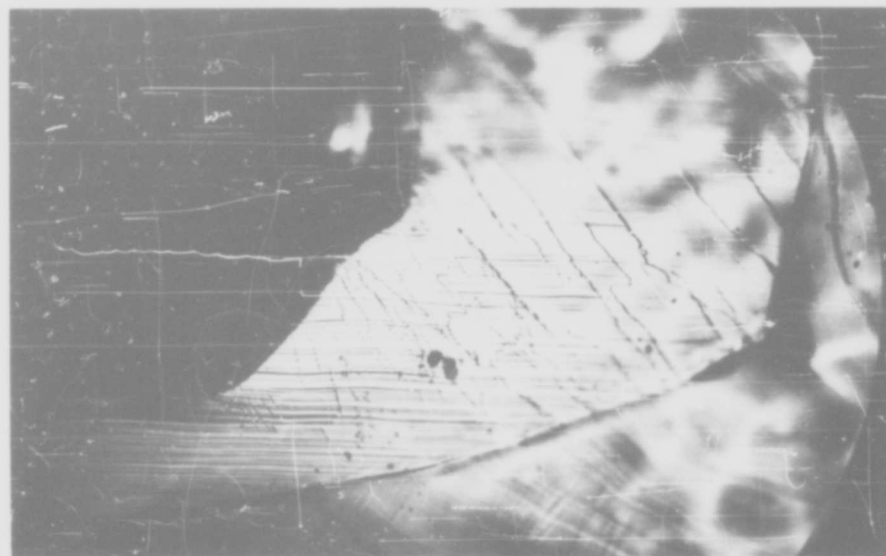


Fig. 20 Slip traces in cadmium  $\tau$  4.95 per cent magnesium alloy, specimen II-7, tested in tension to fracture at  $-122^{\circ}\text{C}$ . Tensile axis and basal traces horizontal,  $\times 1000$



a)

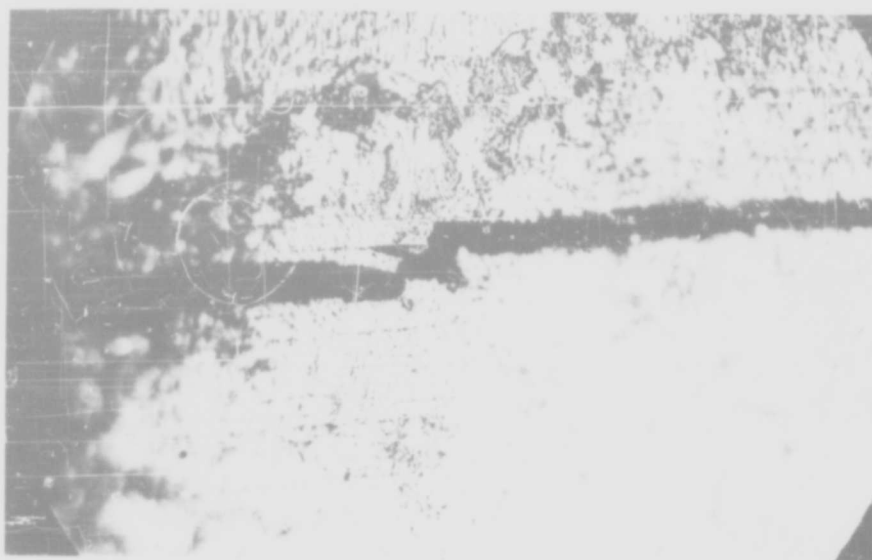


b)

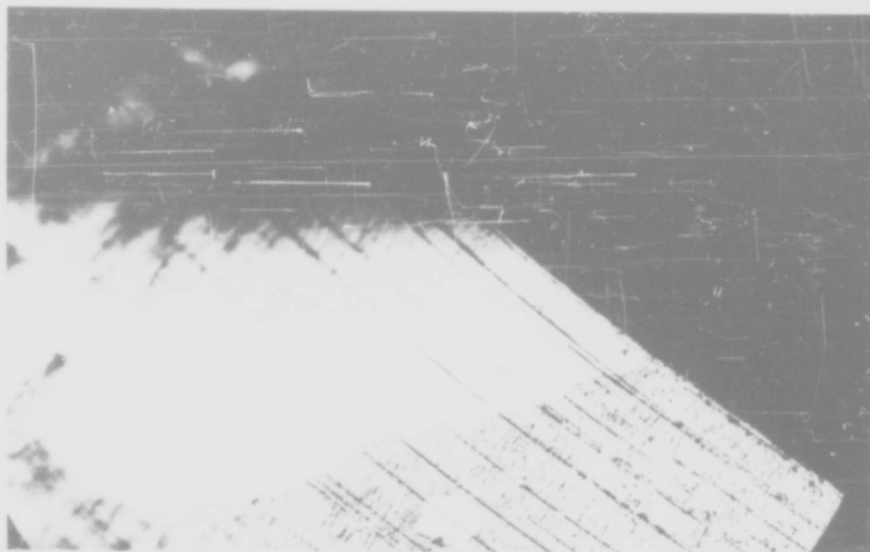
Fig. 21 Transgranular failures in cadmium - 4.95 per cent magnesium alloy, tested in tension a) specimen II-9, room temperature b) specimen II-7,  $-122^{\circ}\text{C}$  x 200



Fig.22 Basal slip and unidentified traces in polycrystalline cadmium, specimen Cd-S-3, strained 15 per cent in compression at  $-196^{\circ}\text{C}$ . Basal traces horizontal, x150



a)



b)

Fig. 23 Basal cleavages in cadmium -15.35 per cent magnesium alloy tested in tension a) specimen VII-6,  $-166^{\circ}\text{C}$ , away from main fracture,  $\times 500$  b) specimen VII-8,  $-126^{\circ}\text{C}$ , part of main fracture,  $\times 200$

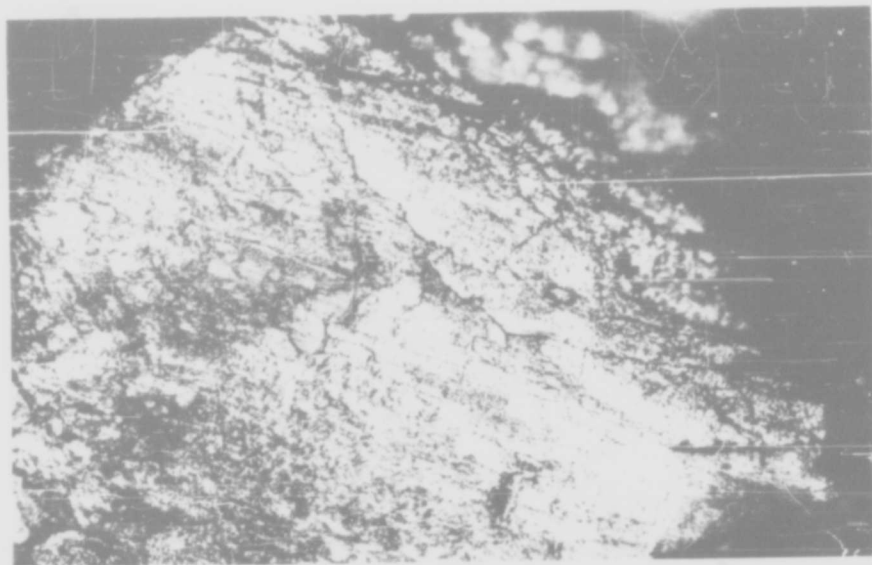


Fig. 24 Cleavage facet in cadmium -15.35 per cent magnesium alloy, specimen VII-2, tested in tension at  $-149^{\circ}\text{C}$ , x100



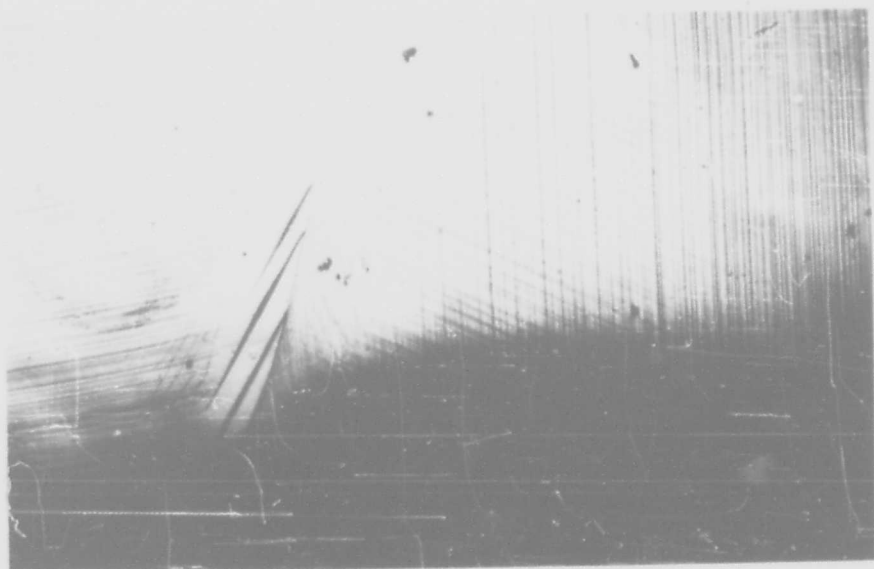


Fig. 25 Slip traces in cadmium-1.96 per cent magnesium alloy, specimen I-G, strained 3 per cent in compression at  $-196^{\circ}\text{C}$ ,  $\times 150$

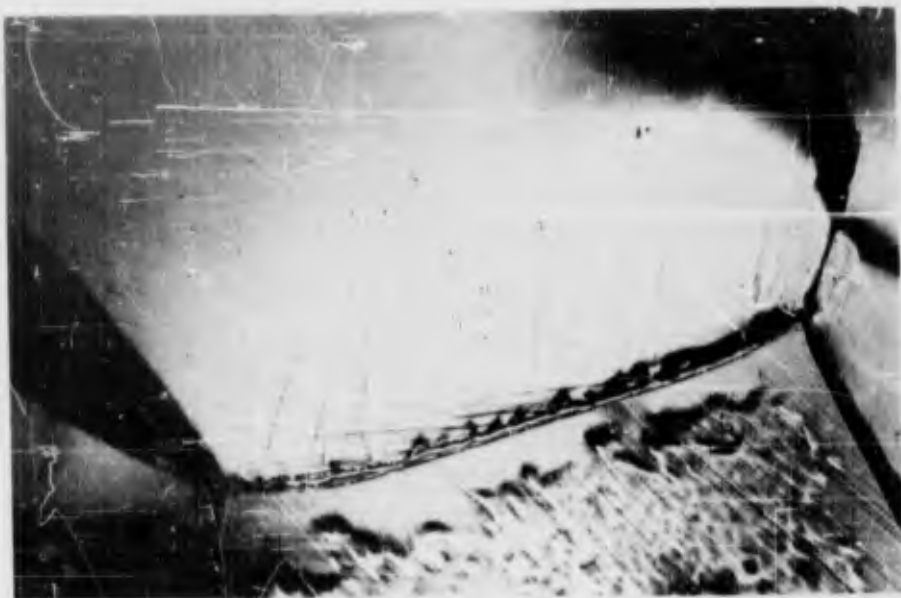
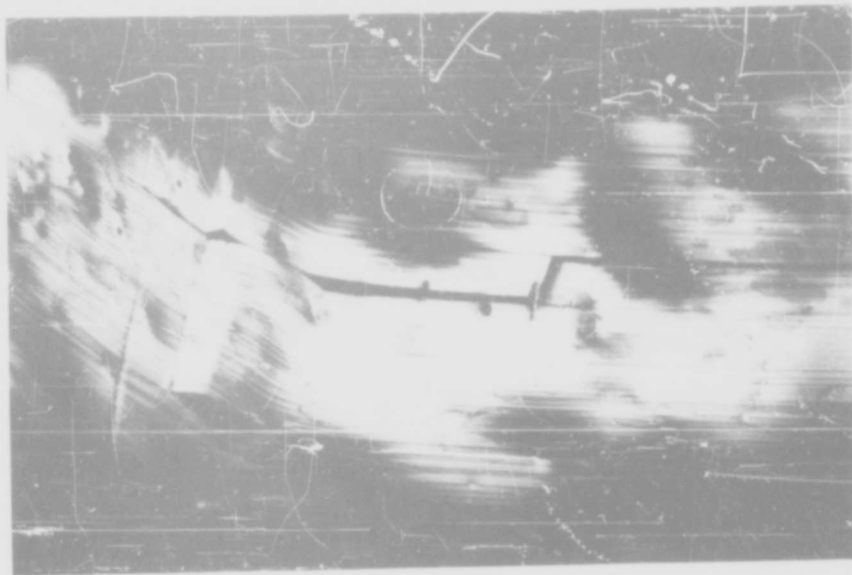


Fig. 26 Slip and twinning in cadmium -4.95 per cent magnesium alloy, specimen II G, strained 8 per cent in compression at room temperature, x150



a)



b)

Fig.27 Cracking along basal planes in kinked region of cadmium  
-3.70 per cent magnesium alloy specimen VIII-1, strained  
20 per cent in compression at room temperature.  
a) x100      b) same region, x250

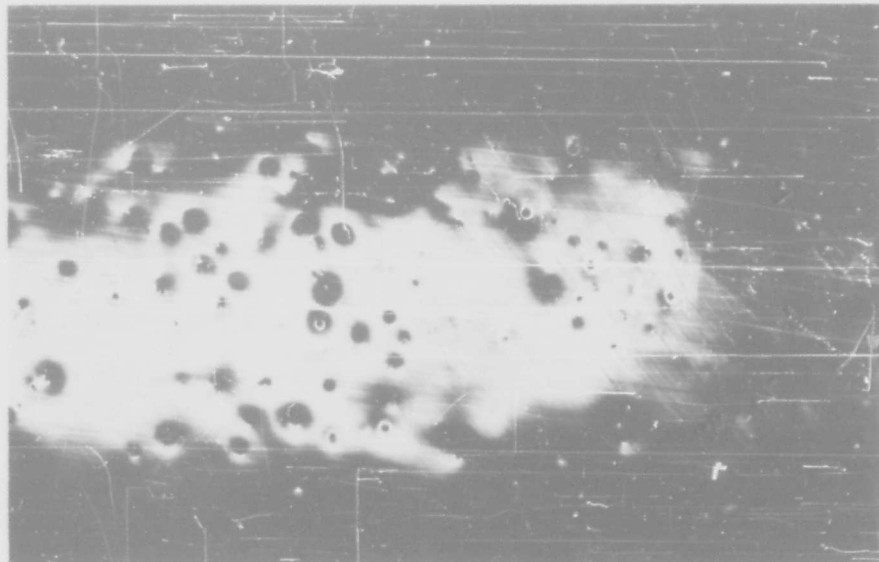
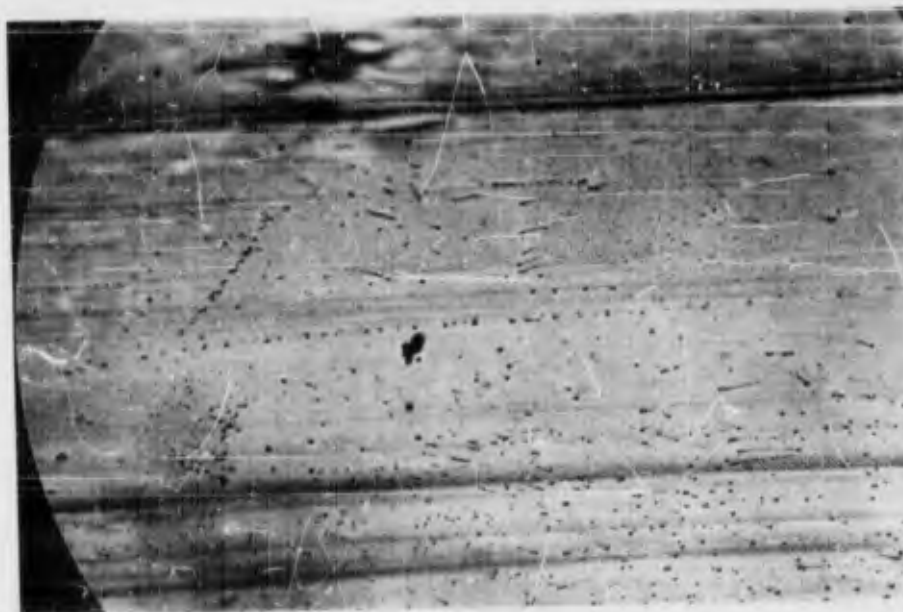


Fig.28 Pyramidal  $\{11\bar{2}2\}$  slip traces in cadmium -3.70 per cent magnesium alloy, specimen VIII - 1, strained 20 per cent in compression at room temperature. Basal slip traces and specimen axis approximately horizontal, x100



a)



b)

Fig.29 Slip traces on single crystal Cd-14-3, tested in tension to first twin burst at 160°C. Specimen axis and basal traces horizontal. a) x150 b)x150

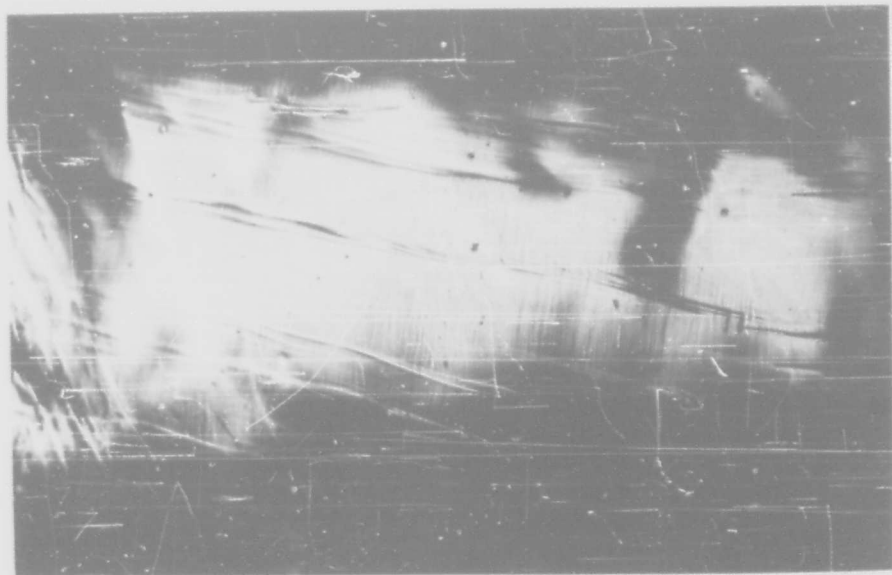
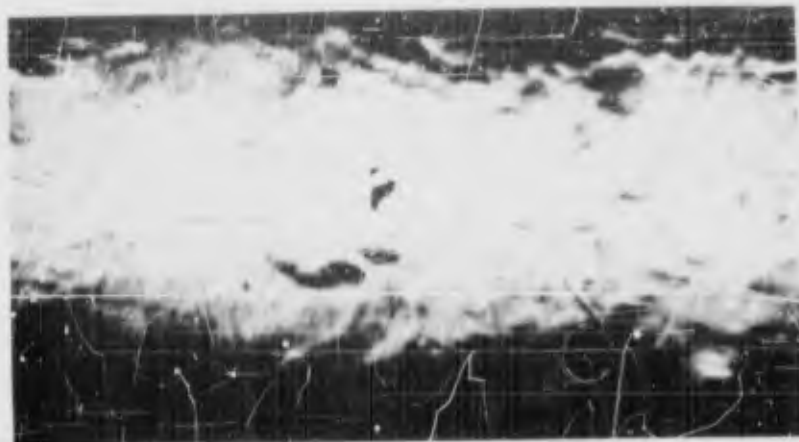


Fig. 30 Pyramidal  $\{11\bar{2}2\}$  slip traces on cadmium tricrystal Cd-40-4, strained 6 per cent in compression at room temperature. Basal traces inclined approximately  $30^\circ$  to horizontal,  $\times 100$



a)



b)

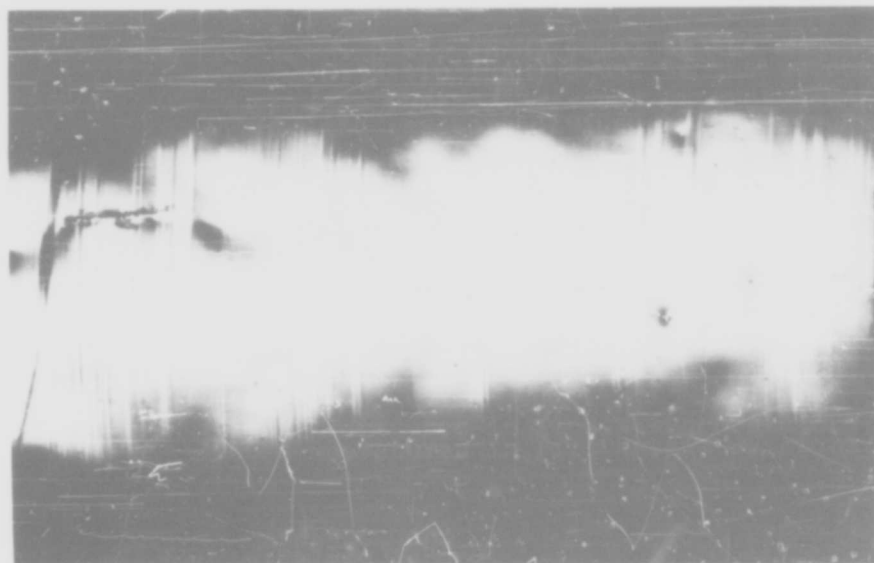


c)

Fig.31 Basal slip and pyramidal  $\{11\bar{2}2\}$  slip in cadmium single crystal Cd-30-3, tested in bending at room temperature. Specimen axis and basal traces horizontal. Note twins and sub-boundary in c)  
 a) x100    b) x150    c) x100



a)



b)

Fig.32 Pyramidal  $\{11\bar{2}2\}$  slip on cadmium bicrystals tested in bending at  $-196^{\circ}\text{C}$ . Specimen axis horizontal, views normal to basal plane. a) specimen Cd-42-1, x200  
b) specimen Cd-42-2, x100





a)



b)



c)

Fig. 33 Pyramidal  $\{11\bar{2}2\}$  slip traces on cadmium bicrystal Cd-44-3, circumferentially scratched with razor blade at various temperatures. Basal slip traces inclined approximately  $20^\circ$  from horizontal. a)  $100^\circ\text{C}$  b)  $22^\circ\text{C}$  c)  $-196^\circ\text{C}$   
xl50

DISTRIBUTION LIST  
FOR  
TECHNICAL NOTES AND TECHNICAL REPORTS

DIRECTORATE OF SOLID STATE SCIENCES

<u>AGENCY</u>	<u>NUMBER OF COPIES</u>
Commander Hq, AF Office of Scientific Research ATTN: SRW Washington 25, D. C.	3
Commander Wright Air Development Center ATTN: WCLJH ATTN: WCLJL ATTN: WCLTL ATTN: WCLTM-1 ATTN: WCLTY-3 Wright-Patterson Air Force Base, Ohio	5
Commander Air Force Cambridge Research Center ATTN: Technical Library ATTN: CRRF L. G. Hanscom Field Bedford, Massachusetts	2
Commander Rome Air Development Center ATTN: Technical Library Griffiss Air Force Base Rome, New York	1
Commander European Office Air Research and Development Command USAF Shell Building, 47 Rue Cantersteen Brussels, Belgium	1
Armed Services Technical Information Agency Arlington Hall Station Arlington 12, Virginia	10

<u>AGENCY</u>	<u>NUMBER OF COPIES</u>
Director of Research and Development Headquarters, United States Air Force ATTN: AFDRD-RE-3 Washington 25, D. C.	1
Commander Army Rocket and Guided Missile Agency Redstone Arsenal, Alabama ATTN: Technical Library	1
Department of the Navy Office of Naval Research ATTN: Code 423 ATTN: Code 421 Washington 25, D. C.	2
Officer in Charge Office of Naval Research Navy No. 100 Fleet Post Office New York, New York	1
Commanding Officer Naval Radiological Defense Laboratory San Francisco Naval Shipyard San Francisco 24, California	1
Director of Army Research Army Research Office Office of the Chief of Research and Development Department of the Army Washington 25, D. C.	1
Division of Research U. S. Atomic Energy Commission Division Office Washington 25, D. C.	1
U. S. Atomic Energy Commission Library Branch Technical Information Division, ORR P. O. Box No. E Oak Ridge, Tennessee	1
Oak Ridge National Laboratory ATTN: Central Files Post Office Box P Oak Ridge, Tennessee	1

<u>AGENCY</u>	<u>NUMBER OF COPIES</u>
Brookhaven National Laboratory ATTN: Research Library Upton, Long Island, New York	1
Argonne National Laboratory ATTN: Librarian P. O. Box 299 Lemont, Illinois	1
Ames Laboratory Iowa State College P. O. Box 14A, Station A	1
Knolls Atomic Power Laboratory ATTN: Document Librarian P. O. Box 1072 Schenectady, New York	1
National Bureau of Standards Library Room 203, Northwest Building Washington 25, D. C.	1
National Science Foundation 1901 Constitution Avenue, N. W. Washington 25, D. C.	1
Director, Office of Ordnance Research Bcm CM, Duke Station Durham, North Carolina	1
Office of Technical Services Department of Commerce Washington 25, D. C.	1
Commander Air Force Ballistic Missile Division (ARDC) ATTN: WDSIT P. O. Box 262 Inglewood, California	1
Document Custodian Los Alamos Scientific Laboratory P. O. Box 1663 Los Alamos, New Mexico	1
Arnold Engineering Development Center ATTN: Technical Library P. O. Box 162 Tullahoma, Tennessee	1

<u>AGENCY</u>	<u>NUMBER OF COPIES</u>
Commanding Officer Ordnance Materials Research Office Watertown Arsenal Watertown 72, Massachusetts	1
Commanding Officer Watertown Arsenal Watertown 72, Massachusetts ATTN: Watertown Arsenal Laboratories Technical Reports Section	
National Aeronautics and Space Administration 1512 H Street, N. W. Washington 25, D. C.	5
Commander Air Technical Intelligence Center ATTN: Deputy for Documentation Wright-Patterson Air Force Base, Ohio	1
Commander Hq. Air Force Office of Scientific Research ATTN: SRIT Technical Library Washington 25, D. C.	2
Commandant AF Institute of Technology ATTN: Technical Library, MCLI Wright-Patterson Air Force Base, Ohio	1
Defense Research Member Canadian Joint Staff ATTN: Mr. H. C. Oatway Director of Engineering Research Defense Research Board Ottawa, Canada THRU: Foreign Release Branch (WCOSR) Wright Air Development Center Wright-Patterson AFB, Ohio	1
Dr. D. F. Bleil Associate Technical Director for Research U. S. Naval Ordnance Laboratory White Oak Silver Spring, Maryland	1
Office of Naval Research Branch Office, London Navy 100, Box 39 FPO New York, N. Y.	15

<u>AGENCY</u>	<u>NUMBER OF COPIES</u>
George Hahn Massachusetts Institute of Technology 8-402 Cambridge 39, Massachusetts	1
Dr. G. B. Greenough Windscale Works Sellafield Calderbridge, Cumberland, England	1
Dr. D. S. Clark Department of Mechanical Engineering California Institute of Technology Pasadena 4, California	1
Dr. A. G. Guy School of Chemical and Metallurgical Engineering Purdue University Lafayette, Indiana	1
Dr. D. Rosenthal Department of Engineering University of California Los Angeles 24, California	1
Professor R. A. Huggins Department of Metallurgical Engineering Stanford University Stanford, California	1
Dr. D. G. Bennett Department of Ceramic Engineering University of Illinois Urbana, Illinois	1
Dr. J. O. Brittain Department of Metallurgy Northwestern University Evanston, Illinois	1
Dr. J. H. Weiner Department of Civil Engineering Columbia University New York 27, New York	1
Professor M. E. Fine Graduate Department of Metallurgy Northwestern University Evanston, Illinois	1

UNCLASSIFIED

UNCLASSIFIED